

Phase Separation Suppression of MOVPE $\text{In}_x\text{Ga}_{1-x}\text{N}$ ($x\sim 0.4$) Epitaxial Layer: A Detail Study and Estimation of Growth Conditions

By

Md.A.Hamid Howlader

A project submitted in partial fulfillment of the requirements for the degree of
M.Sc.Engineering in Dept. of Electrical and Electronic Engineering



Department of Electrical and Electronic Engineering

Khulna University of Engineering & Technology

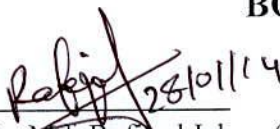
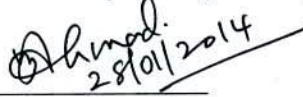

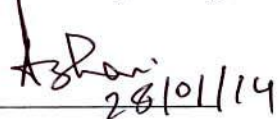
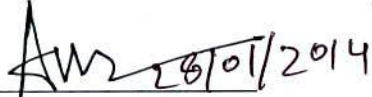
Khulna 9203, Bangladesh

January 2014

Approval


This is to certify that the project work submitted by **Md. A. Hamid Howlader** entitled "*Phase Separation Suppression of MOVPE $In_xGa_{1-x}N$ ($x \sim 0.4$) Epitaxial Layer: A Detail Study and Estimation of Growth Conditions*" has been approved by the board of examiners for the partial fulfillment of the requirements for the degree of M.Sc. Engineering in the Department of Electrical and Electronic Engineering, Khulna University of Engineering & Technology, KUET, Khulna-9203, Bangladesh in January 2014.


BOARD OF EXAMINERS

1.  28/01/14
Prof. Dr. Md. Rafiqul Islam (2)
Department of Electrical and Electronic Engineering
Khulna University of Engineering & Technology
Chairman
(Supervisor)
2.  28/01/2014
Prof. Dr. Mohiuddin Ahmad
Head, Department of Electrical and Electronic Engineering
Khulna University of Engineering & Technology
Member
3.  28-01-2014
Prof. Dr. Md. Rafiqul Islam (1)
Department of Electrical and Electronic Engineering
Khulna University of Engineering & Technology
Member
4.  28/01/14
Prof. Dr. Ashrafal Ghani Bhuiyan
Department of Electrical and Electronic Engineering
Khulna University of Engineering & Technology
Member
5.  28/01/2014
Prof. Dr. Md. Anwarul Abedin
Department of Electrical and Electronic Engineering
Dhaka University of Engineering & Technology, Gazipur
Member
(External)

Declaration

This is to certify that the project work entitled "*Phase Separation Suppression of MOVPE $In_xGa_{1-x}N$ ($x \sim 0.4$) Epitaxial Layer: A Detail Study and Estimation of Growth Conditions*" has been carried out by **Md. A. Hamid Howlader** in the Department of Electrical and Electronic Engineering, Khulna University of Engineering & Technology, Khulna, Bangladesh. The above project work or any part of this work has not been submitted anywhere for the award of any degree or diploma.


Signature of Supervisor


Signature of Candidate

ACKNOWLEDGEMENT

All approvals belong to the Almighty Allah, the most kindhearted and bounteous to all His creatures and their actions. The author gratefully express his deepest sense of gratitude and profound indebtedness to his thesis supervisor, **Dr. Md. Rafiqul Islam**, Professor, Dept. of Electrical and Electronic Engineering, Khulna University of Engineering & Technology (KUET), Bangladesh, for his continuous supervision, encouragements, precious guidance, advices and helps, constructive criticisms and keen interests throughout the progress of the work. The author believes that work with him is a grand opportunity and would be a never-ending memory. The author is grateful and express special thanks to Dr. Ashraful Ghani Bhuiyan and Dr. Md. Rafiqul Islam, Professor, Dept. of Electrical and Electronic Engineering, Khulna University of Engineering & Technology (KUET), Bangladesh, for their adorable attitude, precious mental support and lend a hand to make successful this project. The author also gratefully acknowledges Prof. Dr. Mohiuddin Ahmad, Head, Dept. of Electrical and Electronic Engineering, Khulna University of Engineering & Technology (KUET), Bangladesh, for providing all sorts of facilities to finish this work in time. The authors are also indebted to all the teachers in the Dept. of Electrical and Electronic Engineering for their valuable counseling and constructive criticisms at every stages of the work, which helped him a lot to complete this study in time.

Last but not least, the authors solemnly acknowledges his parents and all the family members, who gave him the utmost mental and financial supports throughout his whole student life and make a way to build up his career in the field of Electrical and Electronic Engineering.

January, 2014

Md. A. Hamid Howlader

Abstracts

Phase Separation Suppression of MOVPE $\text{In}_x\text{Ga}_{1-x}\text{N}$ ($x\sim 0.4$) Epitaxial Layer: A Detail Study and Estimation of Growth Conditions

$\text{In}_x\text{Ga}_{1-x}\text{N}$ is one of the most advantageous materials for high performance electronic and optoelectronic devices. So a demanding analysis has been a central issue for the growth of $\text{In}_x\text{Ga}_{1-x}\text{N}$ to get it as better quality and phase separation free material. It is vital to determine the dependence of the quality and characteristics of epitaxial film on different growth parameters. For this effort, a model has been developed by using the thermodynamic and compositional analysis. The results obtained from this model has been compared and fitted with experimentally obtained data through XRD, RSM, PL, SEM etc. It has also been developed another model on the basis of previous model for growth rate concerning with ammonia flow rate, pressure in addition with different growth parameters. Both of these models are considered for $\text{In}_x\text{Ga}_{1-x}\text{N}$ film on GaN template with an In mole fraction up to 0.4 by Metal Organic Vapor Phase Epitaxy (MOVPE). To understand the effect of strain on phase separation it has been build up a relationship showing the dependence of strain on film thickness and In incorporation in the epitaxial film. To evaluate its perfectness, the result has been compared with the Matthews, Mader and Light Kinetic model for lattice relaxation. Finally three phase diagrams have been developed to optimize the various growth parameters in order to grow phase separation free material. The first phase diagram has been proposed to interpret the phase separation and In content evolution under the influence of growth temperature and precursor gas flow. The second phase diagram has been wished for choosing the value of growth rate to grow up better quality $\text{In}_x\text{Ga}_{1-x}\text{N}$ material. The last one has been developed to include the critical thickness in binodal and spinodal decomposition curve of $\text{In}_x\text{Ga}_{1-x}\text{N}$.

*This work is dedicated to my loved Father, Praiseworthy Mother and Dr. Md. Rafiqul Islam
for guiding me with love and patience*

Contents

	Page
Acknowledgement	i
Abstract	ii
Contents	iv
List of Tables	vii
List of Figures	vii
Nomenclature	ix

CHAPTER I

Introduction

1.1 Research Background	1
1.1.1 Phase Separation and its Impact on Device Performance	2
1.2 Phase Separation Suppression and Thesis Motivation	5
1.3 Objectives of the Thesis	5
1.4 Synopsis of the Thesis	6

CHAPTER II

Literature Review

2.1 Introduction	7
2.2 Structural and Physical Properties of $\text{In}_x\text{Ga}_{1-x}\text{N}$ Film	7
2.2.1 Structure of III-Nitrides	8
2.2.2 Material Characteristics of Wurtzite GaN and InN	9
2.2.4 $\text{In}_x\text{Ga}_{1-x}\text{N}$ Ternary Alloy	10
2.2.5 Strain in $\text{In}_x\text{Ga}_{1-x}\text{N}$ Ternary Alloy	10

	Page
2.3 Challenges in $\text{In}_x\text{Ga}_{1-x}$ Growth	12
2.3.1 Substrates Quality	12
2.3.2 Growth Temperature and V/III Ratio	13
2.3.3 Nitrogen Source	14
2.3.4 Carrier Gas	14
2.4 $\text{In}_x\text{Ga}_{1-x}\text{N}$ Growth Techniques	15
2.4.1 Chemical Vapor Deposition (CVD)	15
2.4.2 Metal-Organic Vapor Phase Epitaxy (MOVPE)	16
2.4.3 Growth of $\text{In}_x\text{Ga}_{1-x}\text{N}$ Epilayer by MOVPE	17
2.4.4 Growth Temperature	18
2.4.5 Molar Ratio	19
2.4.6 TMI Flow Rate	19
2.4.7 Film Thickness	19
2.4.8 Growth Rate	20
2.5 Thermodynamic Analysis of $\text{In}_x\text{Ga}_{1-x}\text{N}$	21
2.5.1 Gibbs' Free Energy and Equilibrium Criteria	21
2.5.2 Gibbs Free Energy of Binary Systems	22
2.5.3 Phase Diagram of $\text{In}_x\text{Ga}_{1-x}\text{N}$ Alloy	27
2.6 Strained Films and Critical Thickness	30
2.6.1 Different Models of Critical Thickness	30
2.6.2 Matthews and Blakeslee	31
2.6.3 People and Bean	32

CHAPTER III Modeling for Growth Conditions of $\text{In}_x\text{Ga}_{1-x}\text{N}$ Epitaxial Layer

	Page
3.1 Introduction	34
3.2 Mathematical Modeling of Growth Condition	34
3.2.1 Modeling Assumption	35
3.2.2 Modeling	35
3.2.3 Effect of Temperature on Growth Rate	40
3.2.4 Effect of Pressure on Growth Rate	41
3.2.5 Effect of V/III ratio on Growth Rate	41
3.3 Theoretical Investigation for Growth Temperature	42
3.4 Strain and Compositional Analysis	44

CHAPTER IV Results and Discussion

4.1 4.1 Introduction	47
4.2 Temperature Dependence of Indium Composition in $\text{In}_x\text{Ga}_{1-x}\text{N}$ Epitaxial Film	47
4.3 Phase Diagram	48

CHAPTER V Conclusion and Future work

5.1 Conclusion	52
5.2 Future Work	53

LIST OF TABLES

Table No	Description	Page
2.1	Lattice parameters of nominally strain-free GaN and InN	10
2.2	Lattice mismatch and thermal expansion coefficient mismatch of GaN with common substrate	12
3.1	Typical values of growth rate and other growth parameters used in different literatures	39

LIST OF FIGURES

Figure No	Description	Page
1.1	Band gap and corresponding wavelength as a function of lattice constant	2
1.2	Configurations for (a) uniform and (b) a phase-separated models in $\text{In}_{0.5}\text{Ga}_{0.5}\text{N}$	3
1.3	Summary of X-ray diffraction data for $\text{In}_x\text{Ga}_{1-x}\text{N}$ grown by MOCVD with indium	4
1.4	Schematic comparison of band structures	4
2.1	Atomic arrangement in tetrahedrally coordinated nitride	8
2.2	Top-view and two side-views of the wurtzite structure	9
2.3	Schematic illustration showing the wurtzite lattice structure	9
2.4	$\text{In}_x\text{Ga}_{1-x}\text{N}$ unit cell under biaxial strain which acts in the basal plane	11
2.5	Schematic illustration of the key CVD steps during deposition	16
2.6	Schematic diagram of MOVPE	17
2.7	Schematic diagram of the cross section of the reactor	18
2.8	PL obtained for $\text{In}_x\text{Ga}_{1-x}\text{N}$ with variable thickness	20
2.9	ω - 2θ x-ray diffraction spectra of (002) plane of $\text{In}_{0.65}\text{Ga}_{0.55}\text{N}$ alloys	20
2.10	The Gibbs free energy for a binary alloy	25
2.11	The enthalpy, entropy, and Gibbs free energy of mixing of $\text{In}_x\text{Ga}_{1-x}\text{N}$ calculated	26
2.12	Gibbs free energy of mixing for a regular solution calculated from equation (2.16)	27
2.13	Binodal (solid) and spinodal (dashed) curves for the $\text{In}_x\text{Ga}_{1-x}\text{N}$ alloys	28
2.14	T-x phase diagram of ternary $\text{In}_x\text{Ga}_{1-x}\text{N}$ alloys for strained layers with the interface orientation perpendicular to the hexagonal axis of the crystal	29

Figure No	Description	Page
2.15	T-x phase diagram of ternary $\text{In}_x\text{Ga}_{1-x}\text{N}$ alloys for strained layers with the interface Orientation parallel to the hexagonal axis of the crystal	29
3.1	Structure of hetero-epitaxial growth $\text{In}_x\text{Ga}_{1-x}\text{N}$	35
3.2	Indium composition depending on TMI flow rate and temperature	36
3.3	In composition in the epitaxial layer as a function of molar ratio	37
3.4	In composition in the epitaxial layer as a function of molar ratio	40
3.5	Growth rate dependence on growth temperature with considering growth pressure and V/III ratio	41
3.6	Growth rate dependency on V/III ratio with considering growth temperature and growth pressure	42
3.7	Dependency of composition (x) on the growth temperature of $\text{In}_x\text{Ga}_{1-x}\text{N}$	43
3.8	Plotting and modelling of In-plane strain in $\text{In}_x\text{Ga}_{1-x}\text{N}$ epitaxial layer	45
3.9	In plane strain variation with Epilayer thickness and the verification of developed model	46
4.1	Indium composition in the epitaxial film for different temperatures and TMI / (TMI+TEG)	47
4.2	Phase diagram for the growth of $\text{In}_x\text{Ga}_{1-x}\text{N}$ concerning molar ratio, Indium composition and growth temperature	48
4.3	Favorable growth region as a function of different particular growth temperatures, group-III flow rate and molar ratio	50
4.4	Phase diagram of the Spinodal decomposition in $\text{In}_x\text{Ga}_{1-x}\text{N}/\text{GaN}$ epitaxial film of different thickness for strained and relaxed condition	51

NOMENCLATURE & ABBREVIATIONS

Symbol	Description
XRD	X-Ray Diffraction
RSM	Reciprocal Space Mapping
PL	Photoluminescence
CVD	Chemical Vapor Deposition
MOVPE	Metal-Organic Vapor Phase Epitaxy
MBE	Molecular Beam Epitaxy
HVPE	Hydride Vapor Phase Epitaxy
MJ	Multi junction
LED	Light Emitting Diode
TMI	Trimethylindium
TEG	Triethylgallium
NH ₃	Ammonia
MR	Molar Ratio
TE	Thermoelectric
MFC	Mass Flow Controller

Chapter 1

Introduction

1.1 Research Background

In the last 25 years, it has been shown that nitride based semiconductor devices are not just only promising but also very applicable in many of modern technologies. The III-Nitride compound semiconductors are recognized as advanced materials because of their different attention-grabbing properties such as direct band gap tunability from 0.7 (InN) to 6.2 eV (AlN) [1], piezoelectricity, polarization, large breakdown voltage, high chemical and thermal stability etc. Depending on the composition and structure as well as combining with nanotechnology group-III nitrides compound semiconductors has become ideal for many applications, including light emitting diodes (LED) and lasers [2]. According to the strong demand of the LED industry, one of today's most prominent materials for producing photonic devices operating in green-blue –ultra violet region is indium gallium nitride ($\text{In}_x\text{Ga}_{1-x}\text{N}$). $\text{In}_x\text{Ga}_{1-x}\text{N}/\text{GaN}$ heterostructure with blue and green color light emitting diodes(LEDs) have been commercialized with excellent efficiency [3], to facilitate the solid-state display with outstanding brightness and contrast. Besides, the band gap of $\text{In}_x\text{Ga}_{1-x}\text{N}$ alloy is potentially tunable from 0.7eV to 3.4eV, covering entire solar spectrum from infrared (IR) to ultraviolet (UV). A continuum of band gaps can be obtained by changing the compositions of In of that alloy. It is a favorable material for future multi junction (MJ) solar cells with momentarily high conversion efficiency [1,4,5]. Also this alloy is used in direct hydrogen generation from aqueous solution of water by photoelectro-chemical effect [6] and has less radiation damage than other photovoltaic materials that are commonly used today in that field [7].

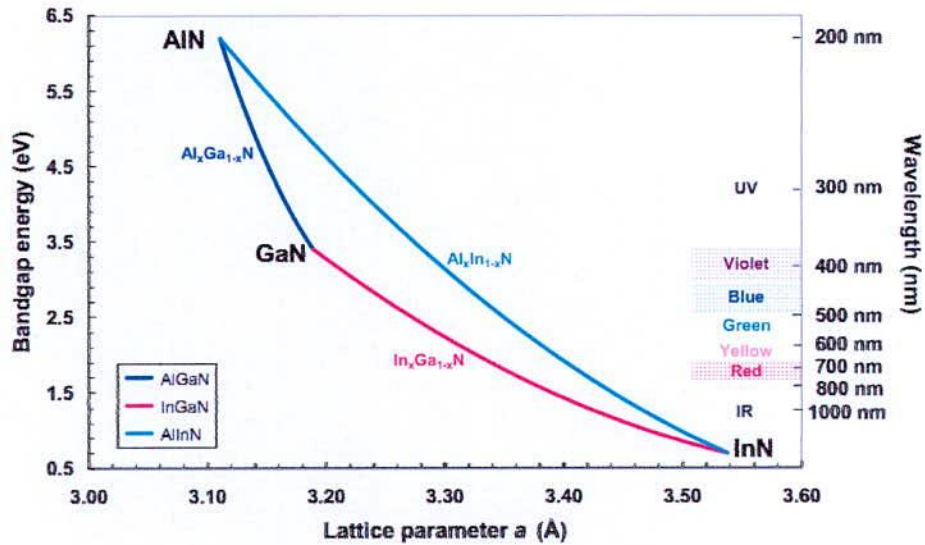


Fig 1.1: Band gap and corresponding wavelength as a function of lattice constant.

Regardless of these encouraging prospects in device fabrication, many problems remain in the growth of $\text{In}_x\text{Ga}_{1-x}\text{N}$ epilayer, especially grown in MOVPE. Growth of $\text{In}_x\text{Ga}_{1-x}\text{N}$ is much more complicated by the fact that the indium incorporation in the film is not a simple function considering the relative input flow of Trimethylindium (TMI) and Triethylgallium (TEG). Also, the thermal decomposition of InN bond and reevaporation from surface leads to indium segregation during the growth of $\text{In}_x\text{Ga}_{1-x}\text{N}$ epitaxial film [8]. The most important delinquent in $\text{In}_x\text{Ga}_{1-x}\text{N}$ is phase separation. The performance of devices is greatly affected by phase separation which indicates the poor material quality. To improve the material quality for better device performance, various growth parameters such as group-III flow rate, group-V flow rate, molar ratio, growth rate, growth pressure and temperature, Indium composition etc. in the epitaxial film must be analyzed and optimized to grow the phase separation free $\text{In}_x\text{Ga}_{1-x}\text{N}$ epitaxy.

1.1.1 Phase Separation and its Impact on Device Performance

The compositional instability or inhomogeneity in an alloy is known as phase separation which leads to the formation of In-rich and/or Ga-rich regions in the epitaxy. The phase separation in $\text{In}_x\text{Ga}_{1-x}\text{N}$ alloy was first observed in an early (1975) experiment in which $\text{In}_x\text{Ga}_{1-x}\text{N}$ samples were annealed in argon ambient at various temperatures below 700°C [9]. Due to phase separation different microstructure and macrostructure

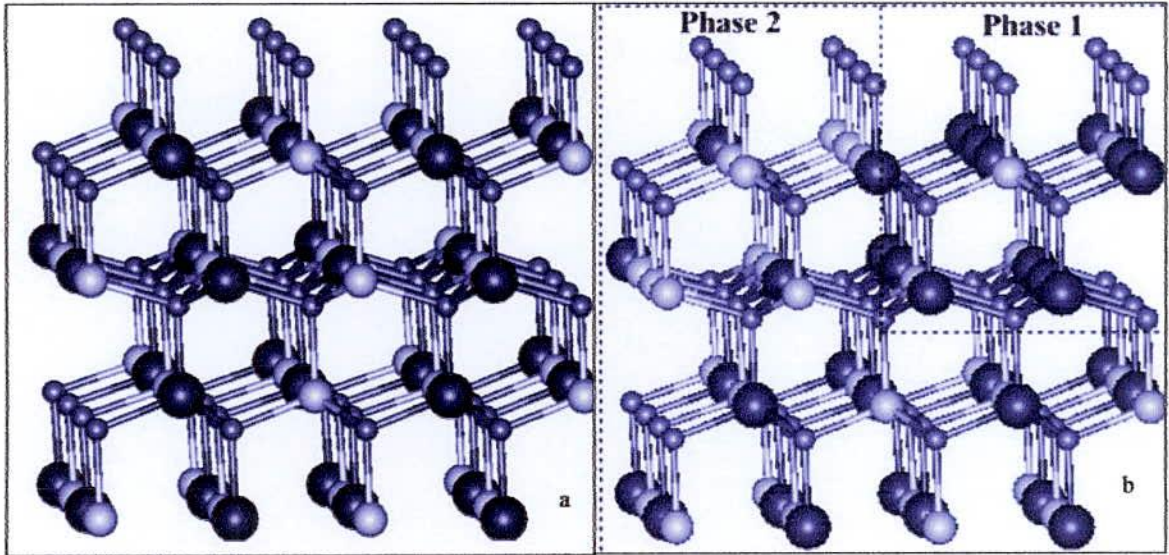


Fig. 1.2 Configurations for (a) uniform and (b) a phase-separated models in $\text{In}_{0.5}\text{Ga}_{0.5}\text{N}$, the $\text{In}_{0.75}\text{Ga}_{0.25}\text{N}$ (25%) and $\text{In}_{0.25}\text{Ga}_{0.75}\text{N}$ (75%) phases are separated by the dash lines and denoted as phase 1 and phase 2, respectively, in (b). (● In ● Ga ● N) [10].

regions of different compositions of the constituent elements are formed. To understand these structures occurred due to phase separation, a larger super cell of 128 atoms is used to construct different In atom distributions. Although it is impossible to go through all the possible configurations, it has been construct clustered and phase-separated distribution as shown in Fig. 1.2(a)–(b) with typical composition $x = 0.5$.

In other words, the formation of microscopic or macroscopic domains of variable constituent composition in a material is known as phase separation. There exists of a solid phase miscibility gap in the $\text{In}_x\text{Ga}_{1-x}\text{N}$ alloy due to the large difference in the lattice constants between GaN and InN, which is also the probable cause of multiple phases and consequent multi-peak luminescence observed in the material [11-12].

Phase separation is usually identified as secondary peaks in addition to the primary peak corresponding to the bulk material during photoluminescence and higher degrees of phase separation are also identified via X-ray diffraction (XRD) as shown in Fig. 1.3.

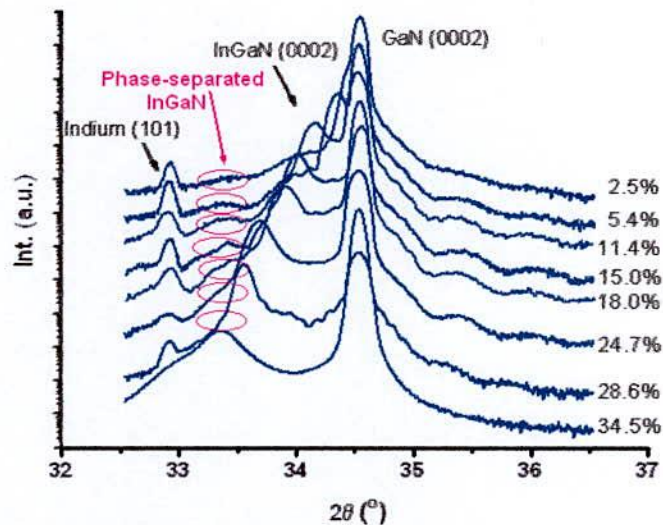


Fig. 1.3: Summary of X-ray diffraction data for InGaN grown by MOCVD with indium composition ranging from 0 to 35% [13].

In order to fabricate high performance devices, the $\text{In}_x\text{Ga}_{1-x}\text{N}$ epitaxial layer must be phase separation free because phase separated material incorporates the band gap energy as shown in Fig.1.4 which sharply affects the performance of electronic and optoelectronic devices. Phase separation, great challenge for the growth of $\text{In}_x\text{Ga}_{1-x}\text{N}$ epitaxy, tends to reduce the short circuit current as well as pin down the open circuit voltage of solar cell which greatly affects the performance criteria. The performance of LED and LESER is also greatly affected by phase separation.

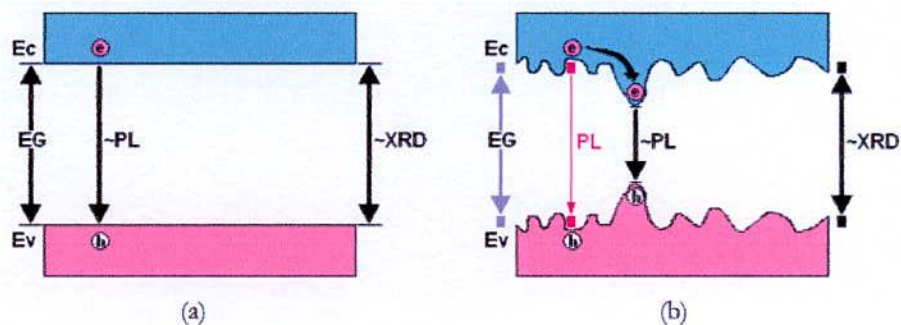


Fig. 1.4: Schematic comparison of band structures of (a) an ideal material, and (b) a phase separated material [13].

1.2 Phase Separation Suppression and Thesis Motivation

In order to suppress the phase separation in $\text{In}_x\text{Ga}_{1-x}\text{N}$ epitaxial layer many approaches are available in the literature. One possible technique is the controlling of various growth parameters. The growth parameters that greatly affect the epitaxial film quality and characteristics are precursor flow rates, growth temperature and pressure, V/III ratio, growth rate, In composition in the epitaxial film etc. [9]. By considering these parameters, phase separation in $\text{In}_x\text{Ga}_{1-x}\text{N}$ epitaxial layer can be suppressed effectively. Another possible method is accumulating additional elastic energy in a uniformly strained epitaxial layer. For coherent layer, as the in-plane strain increases, the excess free energy is decreased by this elastic energy. Strain considerably reduces the phase separation that can be shown as the narrowing of spinodal decomposition region in T-x diagram [14]. The strain also leads to the higher In incorporation in $\text{In}_x\text{Ga}_{1-x}\text{N}$ without phase separation. Various group e.g. Ho and G. B. Stringfellow [11], Yong Huang, et al [15], Md. R. Islam, et al [16] carried out experiment on growth parameters for suppression of phase separation in $\text{In}_x\text{Ga}_{1-x}\text{N}$ epitaxial layer. S. Y. Karpov [14] and recent work by Liu and Zunger [17], show that phase separation may be suppressed by epitaxial strain. Although, a lot of experimental studies exist in the literature, there is no model on MOVPE growth technique by which one can grow phase separation free $\text{In}_x\text{Ga}_{1-x}\text{N}$ film. In this work, a model has been developed so that any researcher can predict about the growth conditions for any arbitrary In composition (0~0.4) before the growth commence.

1.3 Objectives of the Thesis

The goals of this study are to optimize the various growth parameters for suppressing the phase separation and metallic Indium incorporation in $\text{In}_x\text{Ga}_{1-x}\text{N}$ epitaxial film during the growth of $\text{In}_x\text{Ga}_{1-x}\text{N}$ epitaxial layer by MOVPE. The followings are specific aims of this study:

- i. To develop a mathematical model for the $\text{In}_x\text{Ga}_{1-x}\text{N}$ epitaxial layer without phase separation.
- ii. To optimize the various growth parameters for suppressing the phase separation in $\text{In}_x\text{Ga}_{1-x}\text{N}$ epitaxial film by the developed model.

- iii. To develop a mathematical relationship among strain, thickness and composition.
- iv. To anticipate a phase diagram to interpret the phase separation and In content evolution under the influence of different growth parameters.

1.3 Synopsis of the Thesis

This paper consists of five chapters and is mainly focused on the phase separation reduction techniques in $\text{In}_x\text{Ga}_{1-x}\text{N}$ epitaxial layer. An extensive literature survey was carried out during this period of research work to relate the observations with other published results and to identify new frontiers. References are made to acknowledge the work by other authors at the end. The brief summary for each chapter is as given below:

Chapter 1 provides introduction of the study including potential of $\text{In}_x\text{Ga}_{1-x}\text{N}$, statement of the problems. Thesis motivation, objectives along with scope is also highlighted.

Chapter 2 focuses on the available literature related to the thesis topic that would help to understand the thesis. Properties and thermodynamic analysis of $\text{In}_x\text{Ga}_{1-x}\text{N}$ film, brief discussions on several $\text{In}_x\text{Ga}_{1-x}\text{N}$ techniques, and characterization of single phase $\text{In}_x\text{Ga}_{1-x}\text{N}$ alloy were also reviewed in this chapter to conduct the study.

Chapter 3 presents the mathematical modeling of growth conditions for $\text{In}_x\text{Ga}_{1-x}\text{N}$ epitaxial layer in details.

Chapter 4 reveals the results and findings of the study including phase diagram. Finally, some results are compared with experimental work for model verification.

Chapter 5 concludes the thesis work and offers some suggestions which can serve as future problem areas for predecessors.

Chapter 2

Literature Review

2.1 Introduction:

A great problem for the application of III-nitrides in electronic and optoelectronic devices is their tendency toward phase separation [18-26], which can unfavorably affect the alloy electronic and optical properties [27]. The study of the growth parameters and thermodynamics of the $\text{In}_x\text{Ga}_{1-x}\text{N}$ system has great scientific and commercial importance. The growth of high quality $\text{In}_x\text{Ga}_{1-x}\text{N}$ films, especially with compositions above 20% In, is difficult because of phase separation. High temperatures are desirable for growth of nitride films in order to dissociate ammonia (NH_3) and free up nitrogen for bonding. However, the InN bond is significantly weaker than GaN at high temperatures, and $\text{In}_x\text{Ga}_{1-x}\text{N}$ films will tend to have difficulty with In incorporation. If the temperature is lowered, Hydrogen will etch nitrogen away from the In leaving In droplets on the growth surface. In incorporation, and an inherent miscibility gap in the $\text{In}_x\text{Ga}_{1-x}\text{N}$ alloys, can lead to compositional variations and spinodal phase separation over much of the compositional range. Also, large strain energies can be produced in $\text{In}_x\text{Ga}_{1-x}\text{N}$ films grown on GaN, due to the large difference in lattice parameter between GaN and InN.

2.2 Structural and Physical Properties of $\text{In}_x\text{Ga}_{1-x}\text{N}$ Film

It is very important to know about the structural and physical properties of $\text{In}_x\text{Ga}_{1-x}\text{N}$ epitaxial system before the analysis for the phase separation suppression. $\text{In}_x\text{Ga}_{1-x}\text{N}$ is a direct wide band gap semiconductor material consisting of a mixture of two (III)-nitride materials viz. gallium nitride (GaN) and indium nitride (InN). The lateral crystal lattice parameter and corresponding band-gap of $\text{In}_x\text{Ga}_{1-x}\text{N}$ ternary compound depend on In incorporation (x). In this section, the structure and material properties of group (III)-nitrides will be summarized. There will be an overview on strain incorporation in $\text{In}_x\text{Ga}_{1-x}\text{N}$ ternary compounds.

2.2.2 Structure of III-Nitrides

In contrast to other semiconductors, such as silicon or GaAs, bulk single crystals of III-nitrides are not widely available yet. Like most other semiconductor materials, the nitrides have tetrahedrally coordinated atomic arrangements that result in either cubic (zincblende) or hexagonal (wurtzite) lattice structures. For AlN, GaN and InN the zincblende structure is metastable while the wurtzite variant is stable and easier to grow. Therefore, most research has been focused on the wurtzite form which, as a consequence, has given better results up to date for optoelectronic applications. The atomic arrangement of the nitrides can be viewed as consisting of two hexagonal layers. One layer is occupied by nitrogen while the other contains the group III elements. The zincblende structure occurs when the hexagonal layers are stacked in a period . . .ABCABC. . . sequence while the wurtzite structure follows an . . .ABABAB. . . arrangement (see Figure 2.1).

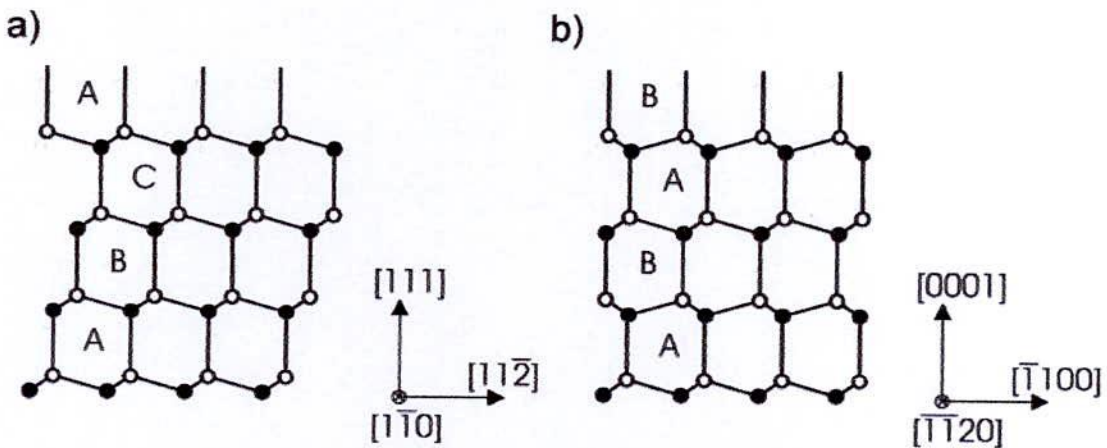


Figure 2.1: Atomic arrangement in tetrahedrally coordinated nitrides: a) cubic zincblende and b) hexagonal wurtzite lattice.

The three-dimensional arrangement of wurtzitic nitrides is shown in Figure 2.2 where one colour (e.g. yellow) represents nitrogen atoms and the other (e.g. red) represents the group-III atoms (Al, Ga or In).

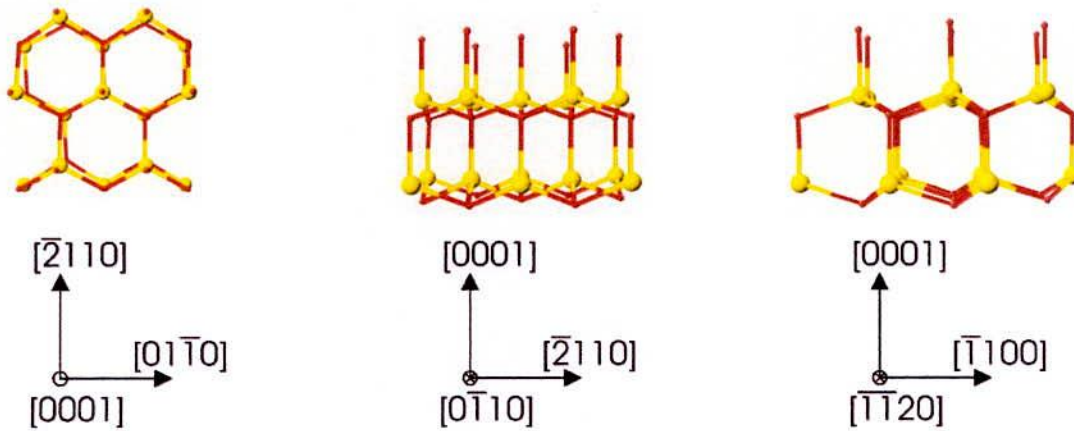


Figure 2.2: Top-view and two side-views of the wurtzite structure

2.2.3 Material Characteristics of Wurtzite GaN and InN

All mechanical properties of GaN and InN used in the subsequent calculations are summarized in this subsection. Lattice parameters of wurtzite GaN and InN are given in Table 2.1 [28]. The lattice parameters for $\text{In}_x\text{Ga}_{1-x}\text{N}$ are derived using Vegard's law, i.e.

$$a = xa_{\text{InN}} + (1-x)a_{\text{GaN}}$$

$$c = xc_{\text{InN}} + (1-x)c_{\text{GaN}}$$

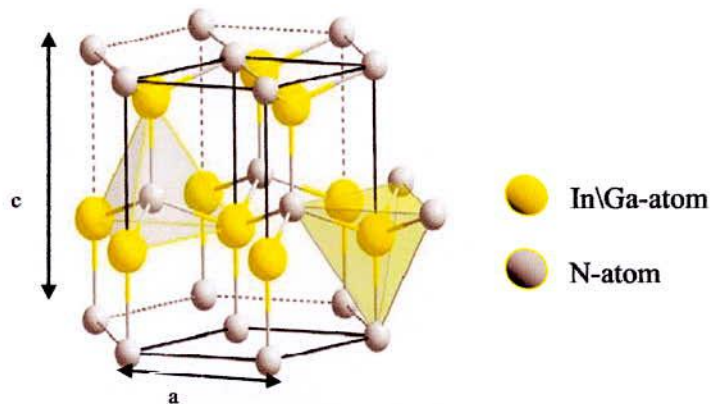


Fig. 2.3: Schematic illustration showing the wurtzite lattice structure.

The strong chemical bonding within III-nitrides results in high melting points, mechanical strength and chemical stability of these materials. Their strong bonding makes them resistant to high-current electrical degradation and radiation damage that is present in the active regions of light emitting devices [28]. These materials also possess good thermal conductivity. III-nitride based devices can operate at high temperatures as well as in hostile environments.

Table 2.1: Lattice parameters of nominally strain free GaN and InN [28].

Material	c[Å]	a[Å]
GaN	5.1855±0.0015	3.1889±0.0015
InN	5.7038±0.0007	3.5377±0.0005

2.2.4 $\text{In}_x\text{Ga}_{1-x}\text{N}$ Ternary Alloy

The $\text{In}_x\text{Ga}_{1-x}\text{N}$ has a great advantage of having the operating wavelength which can be tuned by changing the composition. However, there is a certain limitation of mixing manifested by having the stable and unstable ternary alloy phases depending on the growth temperature and composition of intentional gas phase. Composition and strain can influence the gap bowing [29] and by that change the optical properties of the alloy [30]. Since the effects of the composition and of the strain inside $\text{In}_x\text{Ga}_{1-x}\text{N}$ compound are overlapping and this is further complicated by inter diffusion and phase separation, there is still no clear interpretation of its real structure and the origin of luminescence is an open question [31].

2.2.5 Strain in $\text{In}_x\text{Ga}_{1-x}\text{N}$ Ternary Alloy

The strain plays a massive role in the formation of the $\text{In}_x\text{Ga}_{1-x}\text{N}$ alloy and it has been found that biaxial strain considerably suppresses phase separation. Due to relatively large difference in the lattice parameters of GaN and InN hexagonal unite cells; $\text{In}_x\text{Ga}_{1-x}\text{N}$ films epitaxially grown on a GaN buffer layer are strained. By growth of $\text{In}_x\text{Ga}_{1-x}\text{N}$ in c-direction [0001] on the c-GaN, the in-plane lattice parameter a_{InGa} is compressed trying to adapt to the buffer lattice parameter a_{GaN} as shown in figure 2.4, while the out-of-plane lattice parameter c_{InGa} is expanded.

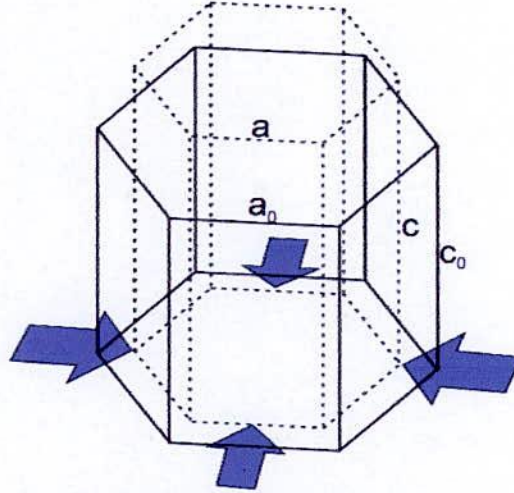


Fig. 2.4 $\text{In}_x\text{Ga}_{1-x}\text{N}$ unit cell under biaxial strain which acts in the basal plane ([32]). a and c denote strained unit cell parameters, while a_0 and c_0 are bulk (relaxed) values.

The in-of-plane strain (ϵ_{\parallel}) and out-of-plane strain (ϵ_{\perp}) are defined through [33]

$$\epsilon_{\parallel} = \frac{a - a_0}{a_0}; \quad \epsilon_{\perp} = \frac{c - c_0}{c_0}$$

Where a and c denoting the strained lattice parameters and a_0 , c_0 the relaxed ones.

To determine the chemical composition, Vegard's Rule [34] is used. It describes how the lattice parameters (a_0 , c_0) change with the chemical composition, x . Neglecting the deviations, it is generally assumed to be linear for the semiconductor alloy systems.

$$a_0(x) = x a_{\text{InN}} + (1 - x) a_{\text{GaN}}$$

$$c_0(x) = x c_{\text{InN}} + (1 - x) c_{\text{GaN}}$$

Where $a_0(x)$ and $c_0(x)$ are the relaxed (or bulk) in-plane and out-of-plane lattice parameters of the $\text{In}_x\text{Ga}_{1-x}\text{N}$ compound.

2.3 Challenges in $\text{In}_x\text{Ga}_{1-x}\text{N}$ Growth

There are several problems to be overcome for high crystalline and phase separation free $\text{In}_x\text{Ga}_{1-x}\text{N}$ film growth. These problems are narrow region of growth temperature due to the low decomposition temperature, low cracking efficiency of NH_3 , no suitable nitrogen precursors to improve the decomposition efficiency of NH_3 , and carrier gas. These problems which occur during the growth of $\text{In}_x\text{Ga}_{1-x}\text{N}$ are briefly discussed in this part.

2.3.1 Substrates Quality

Growth of III-nitride epitaxial layers has been intensively studied due to fundamental challenges associated with obtaining material of high crystallinity. Crystalline perfection of epitaxial structures is one of the main factors that affect the electrical and physical parameters of the material, and consequently, limits their applications.

Table 2.2: Lattice mismatch and thermal expansion coefficient mismatch of GaN with common substrates [12].

Substrate	Lattice mismatch	Thermal expansion coefficient mismatch
Sapphire	16%	-34%
SiC	3%	25%
ZnO	2%	-14%
Si	17%	100%

The III-nitrides typically crystallize in a wurtzite crystal. Sapphire is the most commonly used substrate for the growth of wurtzite $\text{In}_x\text{Ga}_{1-x}\text{N}$. However, due to the large lattice mismatch (16% for GaN on sapphire and 29% for InN on sapphire) and thermal mismatch (-34% for GaN on sapphire and -100% for InN on sapphire) between sapphire and III-Nitrides, epitaxial films on sapphire result in phase separation and high dislocation densities.

As a result it becomes progressively difficult to incorporate higher In compositions in $\text{In}_x\text{Ga}_{1-x}\text{N}$. Moreover, in spite of the advances made in science today, due to unavailability of high quality material, the band gap of InN is still a topic of debate. Consequently, it becomes more difficult to fabricate $\text{In}_x\text{Ga}_{1-x}\text{N}$ solar cells at higher In compositions.

2.3.2 Growth Temperature and V/III Ratio

The growth of InN in $\text{In}_x\text{Ga}_{1-x}\text{N}$ is the most difficult among the III-nitrides because the equilibrium vapor pressure of N_2 over the InN is several orders higher than AlN and GaN [35]. Because of the low InN dissociation temperature and high equilibrium N_2 vapor pressure over the InN in $\text{In}_x\text{Ga}_{1-x}\text{N}$ film [36], the growth of $\text{In}_x\text{Ga}_{1-x}\text{N}$ requires a low growth temperature. Due to the low ($\sim 550^\circ\text{C}$) growth temperature, the MOVPE growth of $\text{In}_x\text{Ga}_{1-x}\text{N}$ is thought to be restricted by a low decomposition rate of NH_3 . Although a higher growth temperature is expected to result in a higher decomposition rate of NH_3 , it can also result in thermal decomposition (thermal etching) of the grown $\text{In}_x\text{Ga}_{1-x}\text{N}$. On the other hand, the growth at a low temperature (lower than 400°C) is dominated by the formation of metallic In droplets due to the shortage of reactive nitrogen. Epitaxial growth at low temperature becomes impossible due to reduced migration of the deposited materials. Therefore, the region suitable for the deposition of $\text{In}_x\text{Ga}_{1-x}\text{N}$ is very narrow. Koukita et al. carried out a thermodynamic study on the MOVPE growth of III-nitrides [37]. They pointed out that a high input V/III ratio, the use of an inert carrier gas, and a low mole fraction of the decomposed NH_3 are required for the growth of InN. High input V/III provides sufficient amount of reactive nitrogen, since the NH_3 decomposition rate is low at low growth temperature. So, a suitable region of V/III ratio and growth temperature is required for the high quality $\text{In}_x\text{Ga}_{1-x}\text{N}$ growth without In droplets formation during the growth.

2.3.3 Nitrogen Source

$\text{In}_x\text{Ga}_{1-x}\text{N}$ is typically grown by MOVPE using conventional group-III precursors such as Trimethylindium (TMI) and Triethylgallium (TEG) with NH_3 as the active nitrogen source. However, InN and $\text{In}_x\text{Ga}_{1-x}\text{N}$ are relatively difficult to produce with the high quality required for minority carrier devices due to high equilibrium N_2 vapor pressure and the low decomposition efficiency of NH_3 as discussed earlier.

NH_3 is almost stable even at 1000 °C and decomposes only 15 % at 950°C, even when catalyzed by GaN [38]. The combination of high growth temperatures and high nitrogen volatility leads to high concentrations of N vacancies in GaN and InN . In spite of these limitations, NH_3 has been still widely used as a nitrogen source. The design of the optimum nitrogen source for the growth of III/V nitrides is still required even though it is tricky.

2.3.4 Carrier Gas

Carrier gas is used as the medium to give the uniform flow pattern of precursors in MOVPE reactor. H_2 and N_2 carrier gas have been usually used in $\text{In}_x\text{Ga}_{1-x}\text{N}$ growth. Koukitu et al. carried out a detailed thermodynamic study on the role of hydrogen during the MOVPE growth of III-nitrides [39]. They showed that increase of hydrogen in the growth system results in a decrease of InN deposition rate in $\text{In}_x\text{Ga}_{1-x}\text{N}$ film (called etching), which they suggested was due to the decrease of driving force for the deposition.

Thus the reaction for the growth of $\text{In}_x\text{Ga}_{1-x}\text{N}$ proceeds more effectively in the inert gas system and is prevented with the increase of H_2 . Therefore it is necessary to use inert carrier gas in the growth of $\text{In}_x\text{Ga}_{1-x}\text{N}$. These theoretical and experimental results confirm that using a N_2 carrier gas is preferred (and widely used) for successful $\text{In}_x\text{Ga}_{1-x}\text{N}$ growth.

2.4 InGaN Growth Techniques

Several methods have been developed for the growth of InGaN epitaxial layer. The choice of which method is used is based on the desired properties of the crystals. In general, two parameters must be considered viz. thickness and quality. They growth techniques are classified as:

(1) Modern technique for epitaxial growth

- (I) MOVPE or MOCVD or OMVPE
- (II) MBE
- (III) HVPE
- (IV) Sputtering
- (V) Pulsed LASER Deposition

(2) Old technique for epitaxial growth

- (I) Reactive Evaporation
- (II) Electron Beam Plasma Technique
- (III) Salvo thermal Method.

2.4.1 Chemical Vapor Deposition (CVD)

CVD involves the dissociation and/or chemical reactions of gaseous reactants in an activated (heated, plasma etc.) environment, followed by the formation of a solid film. The deposition involves homogeneous gas phase reactions, which occur in the gas phase, and heterogeneous chemical reactions which occur on a heated surface leading to the formation of epitaxial films.

In general, the CVD process involves the following key steps as shown in Fig. 2.5 [40,41].

- (1) Generation of active gaseous reactant species.
- (2) Transport of the gaseous species into the reaction chamber.
- (3) Gaseous reactants undergo gas phase reactions forming intermediate species.
- (4) Absorption of gaseous reactants onto the heated substrate, and the heterogeneous reaction occurs at the gas-solid interface (i.e. heated substrate) which produces the deposit and by-product species.

- (5) The deposits will diffuse along the heated substrate surface forming the crystallization centre and growth of the film.
- (6) Gaseous by-products are removed from the boundary layer through diffusion or convection.
- (7) The unreacted gaseous precursors and by-products will be transported away from the deposition chamber

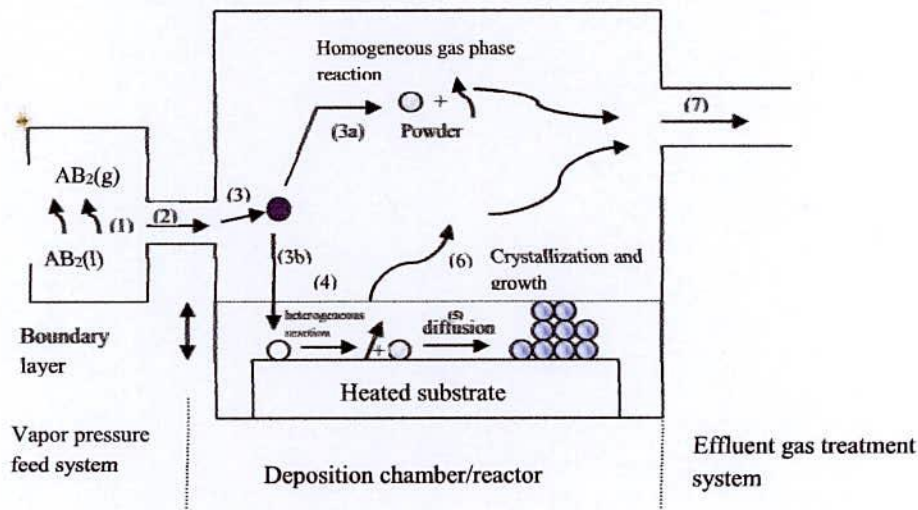


Fig. 2.5: Schematic illustration of the key CVD steps during deposition.

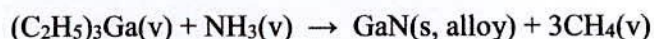
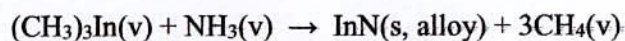
2.4.2 Metal-Organic Vapor Phase Epitaxy (MOVPE)

Metal organic Vapor Phase Epitaxy (MOVPE) is a well-established growth method for the growth of $\text{In}_x\text{Ga}_{1-x}\text{N}$. It is one growth method among CVD, which has been classified according to the use of metal organics as precursors. MOVPE goes by a number of names, including Organometallic Vapor Phase Epitaxy (OMVPE), Metal organic Chemical Vapor Deposition (MOCVD), Organometallic Chemical Vapor Deposition (OMCVD) and occasionally Organometallic Epitaxy (OME). Using nitrogen and/or hydrogen as carrier gas, Metal organic (MO) precursors are used as the metal sources (for example TMG or TEG as a gallium precursor) and ammonia (NH_3) is used as nitrogen source. Both, the metal organic precursor and NH_3 are transported to the reaction zone above a substrate to form the desired group-III nitride

compound. Growth rates as high as 5 $\mu\text{m/hr}$ can be achieved by MOVPE. Major impurities found are oxygen, hydrogen, carbon, and silicon.

2.4.3 Growth of $\text{In}_x\text{Ga}_{1-x}\text{N}$ Epilayer by MOVPE

The MOVPE system used for the growth of GaN or $\text{In}_x\text{Ga}_{1-x}\text{N}$ alloys in this dissertation utilizes Metal organic sources from group III-elements. The formation of solid GaN or InN on the substrate is happened by the following chemical reactions in vapor phase with the organo-metallic reactant species. For this reason it is called metal organic vapor phase Epitaxy.



Where, InN(alloy) and GaN(alloy) stands for the binary compounds in the $\text{In}_x\text{Ga}_{1-x}\text{N}$ alloy.

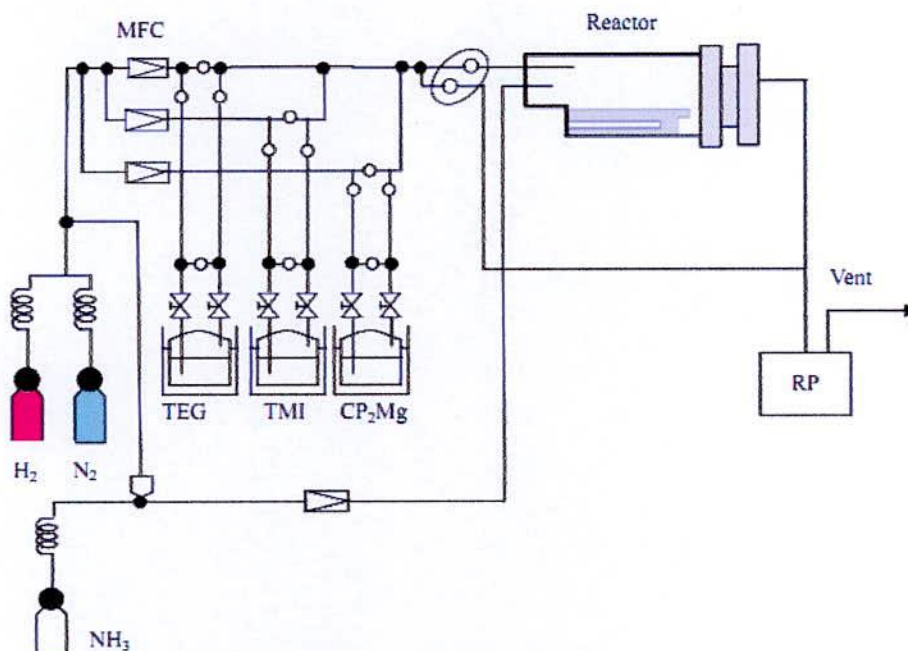


Fig. 2.6: Schematic diagram of MOVPE.

The MOVPE system mainly consists of four main parts: the gas handling system, the reactor, the heating system and the exhaust and vacuum system. The main part of the system is the reactor part where growth reaction takes place. System has a horizontal, circular tube quartz reactor. A high purity carbon susceptor is used to hold the substrate.

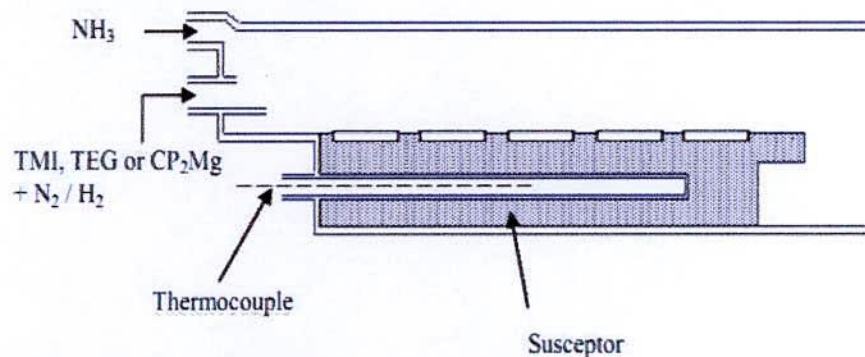


Fig. 2.7: Schematic diagram of the cross section of the reactor.

A (400 ± 30 kHz) RF generator is used to heat up the susceptor. The temperature of the susceptor is measured by an R type thermo-couple (Platinum/Rhodium alloy) inserted in the susceptor through a quartz tube. The temperature is controlled by a temperature controller. To pump down the system to low pressure, a high capacity mechanical pump with oil filter pump was used. A turbo pump coupled into this system is employed to pump down to vacuum before the growth.

2.4.4 Growth Temperature

Growth temperature plays a significant role in indium incorporation as well as phase separation in $\text{In}_x\text{Ga}_{1-x}\text{N}$ film [42]. It has been observed by Rafiqul et al. [16] that the $\text{In}_x\text{Ga}_{1-x}\text{N}$ film grown at 800°C with TMI/(TMI + TEG) molar ratio of 0.38 is without phase separation and metallic In incorporation. It has also been seen that in order to control the In content in the range of 0-0.4, the $\text{In}_x\text{Ga}_{1-x}\text{N}$ film has been grown with the same (0.38) TMI/(TMI + TEG) molar ratio in the temperature of $750^\circ\text{C} \sim 850^\circ\text{C}$.

2.4.5 Molar Ratio

In order to suppress the phase separation and metallic indium formation in $\text{In}_x\text{Ga}_{1-x}\text{N}$, the molar ratio plays a significant role in the growth process of $\text{In}_x\text{Ga}_{1-x}\text{N}$. Molar ratio should not very low to get single phase $\text{In}_x\text{Ga}_{1-x}\text{N}$ alloy. On the other hand, it should not high enough to more than 0.50 due to the utmost risk of In droplet formation. It has been observed by Rafiqul et al. [16] that with molar ratio 0.20 at temperature 800°C there is the presence of another secondary peak of $\text{In}_x\text{Ga}_{1-x}\text{N}$ which represents the phase separation.

2.4.6 TMI Flow Rate

With the increase of TMI flow rate the In composition in the $\text{In}_x\text{Ga}_{1-x}\text{N}$ alloy increases. Low TMI flow rate causes the phase separation in $\text{In}_x\text{Ga}_{1-x}\text{N}$ film as well as reduces In composition [43,44]. So TMI flow rate should not much low rather than sufficient amount to make single phase $\text{In}_x\text{Ga}_{1-x}\text{N}$ alloy. Rafiqul et al.[16] has been shown that at low TMI flow rates (100sccm), the indium composition is only 8% but also a secondary phase-separated domain is generated. They recommended it may be due to the strain state in the material varies to a much greater extent due to the additional gallium species.

2.4.7 Film Thickness

Film thickness of $\text{In}_x\text{Ga}_{1-x}\text{N}$ is one of important parameter in controlling phase separation. With the increase of thickness the film is relaxed and phase separated. Since the material stays in the growth ambient for a longer time for higher thicknesses and it gets enough time to release the biaxial strain and creates the tendency to form phase separated film. It has been observed by Omkar K. Jani [12] from PL mission that secondary $\text{In}_x\text{Ga}_{1-x}\text{N}$ phases are more prominent at higher thicknesses.

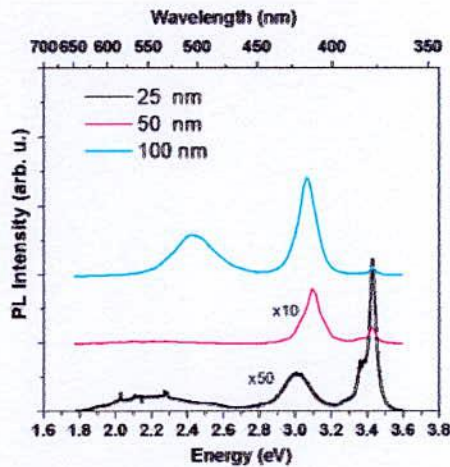


Fig. 2.8: PL obtained for $\text{In}_x\text{Ga}_{1-x}\text{N}$ with variable thickness [39].

2.4.8 Growth Rate

Growth rate is another challenging parameter to generate a single phase $\text{In}_x\text{Ga}_{1-x}\text{N}$ alloy. The growth rate is controlled by III/V ratio. The increase in III sources increases the growth rate and diminishes the phase separation. Thus phase separation can be controlled kinetically, using high growth rate. Bed nidhi et al. [45] has been seen the effect of growth rate on phase separation.

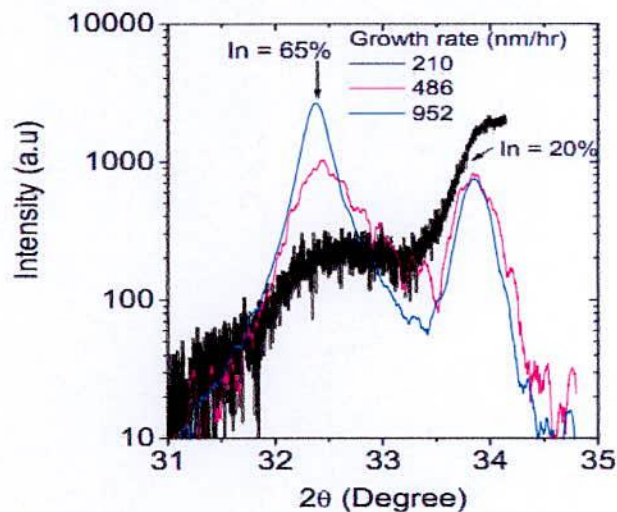


Fig. 2.9: ω - 2θ x-ray diffraction spectra of (002) plane of $\text{In}_{0.65}\text{Ga}_{0.55}\text{N}$ alloys grown at different [45].

In conclusion, in order to get single phase $\text{In}_x\text{Ga}_{1-x}\text{N}$ film or phase separation free film the above parameters should be carefully considered during the growth of $\text{In}_x\text{Ga}_{1-x}\text{N}$ film. Further improvement in material quality is expected by optimizing other growth parameters.

2.5 Thermodynamic Analysis of $\text{In}_x\text{Ga}_{1-x}\text{N}$

2.5.1 Gibbs' Free Energy and Equilibrium Criteria

The most convenient way to measure energy in phase systems is the Gibbs free energy. The Gibbs free energy is normally written as:

$$G = H - TS \dots\dots\dots (2.1)$$

Where, T is the temperature (K), S is the entropy, and H is the enthalpy of the system that is given by:

$$H = U + pV \dots\dots\dots (2.2)$$

In the above equation U is the internal energy of the system, p is pressure and V is volume. The second law of thermodynamics gives the fundamental criterion for equilibrium.

$$dS \geq \frac{dQ}{T} \dots\dots\dots (2.3)$$

We can rewrite the second law in the following form

$$dQ - TdS \leq 0 \dots\dots\dots (2.4)$$

From the first law of thermodynamics with only pV work we have

$$dU = dQ - pdV \dots\dots\dots (2.5)$$

By combining (2.1), (2.2) and (2.5) the change in Gibbs free energy is

$$\begin{aligned} dG &= dH - TdS - SdT \\ &= dQ + pdV + Vdp - TdS - SdT \\ &= dQ - TdS + pdV - SdT \dots\dots\dots (2.6) \end{aligned}$$

For a process at constant temperature and pressure equations (2.4) and (2.6) give

$$dG = dQ - TdS \leq 0 \dots\dots\dots (2.7)$$

It can be seen from equation (2.7) that at constant temperature and pressure the stable state of a system is the one that has the minimum value of the Gibbs free energy. Any spontaneous process in a system at constant T and p must decrease the Gibbs free energy (if the system is away from equilibrium) or leave the Gibbs free energy unchanged (if the system is at equilibrium). Thus, the phase stability in a system can be determined from knowledge of the variations of the Gibbs free energies with composition and temperature of the various possible phases.

2.5.2 Gibbs Free Energy of Binary Systems

(A) Ideal Solutions

In an isobaric and isothermal process of mixing of substances A and B the change in Gibbs free energy as a result of mixing is:

$$dG_{mix} = dH_{mix} - TdS_{mix} \dots\dots\dots (2.8)$$

This dG_{mix} is the difference between the free energy of the solution/mixture and the free energy of the pure components A and B. The enthalpy term, dH_{mix} , represents the nature of the chemical bonding, or, in different words, the extent to which A prefers B, or A prefers A as a neighbor. The entropy term, dS_{mix} , signifies the increase in disorder in the system as we let the A and B atoms mix. It is independent of the nature of the chemical bonding.

An ideal solution is one in which the atoms are randomly mixed and the interactions between species are identical, in other words the bond energy doesn't change whether the bond is A-A, B-B, or A-B. Therefore, for an ideal solution there is no overall enthalpy change. Then the Gibbs free energy of mixing becomes:

$$dG_{mix} = -TdS_{mix} \dots\dots\dots(2.9)$$

Now let's assume we have a crystal with a total of N sites available for the occupation of atoms or molecules, n of which are occupied by A atoms/molecules and $(N - n)$ are occupied by B atoms/molecules. In this case it can be shown that the total number of ways of distributing A and B is given by:

$$w = \frac{N!}{n!(N - n)!} \dots\dots\dots (2.10)$$

The entropy of mixing components A and B is given by Boltzmann's equation

$$dS_{mix} = k_B \ln W \dots\dots\dots (2.11)$$

where k_B is Boltzmann's constant and W is the number of the different arrangements of the atoms on lattice sites of the crystal given by equation (2.10). Replacing W in equation (2.11) gives

$$dS_{mix} = k_B \ln\left(\frac{N!}{n!(N - n)!}\right) \dots\dots\dots (2.12)$$

Using Stirling's approximation $N \ln N! = N \ln N - N$ for large N , equation (2.12) becomes

$$\begin{aligned} dS_{mix} &= k_B [N \ln N - n \ln n - (N - n) \ln(N - n)] = \\ &= -k_B \left[n \ln\left(\frac{n}{N}\right) + (N - n) \ln\left(\frac{N - n}{N}\right) \right] = \dots\dots\dots (2.13) \\ &= -Nk_B \left[\frac{n}{N} \ln\left(\frac{n}{N}\right) + \frac{(N - n)}{N} \ln\left(\frac{N - n}{N}\right) \right] \end{aligned}$$

If we consider N to be Avogadro's number, $N = 6.02 \cdot 10^{23}$ atoms or molecules, Then $N k_B = R = 8.314$ J/mole-K. The mole fractions of components A and B are given by $x_A = n/N$ and $x_B = (N - n)/N$ respectively, so equation (2.13) reduces to

$$dS_{mix} = -R(x_A \ln x_A + x_B \ln x_B) \dots\dots\dots (2.14)$$

This defines the ideal entropy change of mixing. Then the Gibbs free energy of Mixing for an ideal solution is given by:

$$dG_{mix} = RT(x_A \ln x_A + x_B \ln x_B) \dots\dots\dots(2.15)$$

It is clear that in the case of the ideal mixing of two components the change in Free energy dG_{mix} is always negative, since x_A and x_B are always less than unity.

(B) Regular Solutions:

The regular solution model is the simplest model used to describe the thermodynamic properties of semiconductors. A regular solution is a solution that diverges from the behavior of an ideal solution only moderately. The components mix in a completely random manner just like in the ideal solution, so the entropy is still the same as in the ideal mixing. From the Gibbs free energy curve, it is possible to generate the phase diagram for a given system. The Gibbs free energy of mixing for the regular solution model is

$$\Delta G = Wx(1-x) + TR[x \ln(x) + (1-x) \ln(1-x)] \dots\dots\dots(2.16)$$

Where, $W \rightarrow$ interaction parameter (J/mole),

$T \rightarrow$ Temperature (K),

$R \rightarrow$ Gas constant ($\text{JK}^{-1}\text{mole}^{-1}$)

There has two parts in this equation, $Wx(1-x)$ is enthalpy and $TR[x \ln(x) + (1-x) \ln(1-x)]$ is called entropy the summation of enthalpy and entropy is called free energy of mixing or mixing free energy or Gibbs free energy.

In the case where the enthalpy is positive but comparable to the entropy term at a given temperature, the phase diagram is determined by the shape of the free energy curve as the one shown in Fig. 2.1, which is calculated from equation (2.16) for $w = 20 \text{ kJ/mole}$ and $T = 850 \text{ K}$.

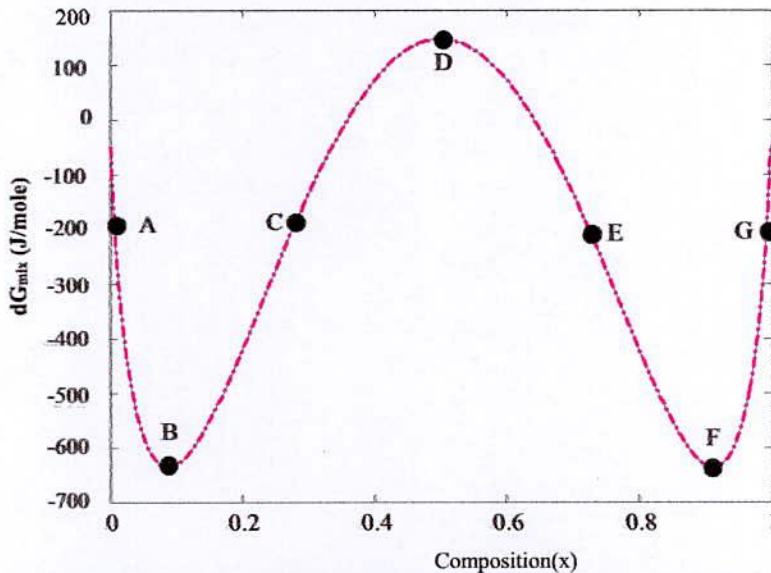


Fig. 2.10 The Gibbs free energy for a binary alloy when the enthalpy of mixing is larger than the entropy term calculated from equation (2.16) for $W = 20 \text{ kJ/mole}$ and $T = 850 \text{ K}$.

The Gibbs free energy curve in Fig. 2.10 shows two minima (points B and F) and a maximum (point D). The minima represent the equilibrium compositions. Any mixture with composition between points B and F will separate into two phases with equilibrium compositions B and F. Any composition within the region between the two equilibrium points is not considered to be at equilibrium. Near the equilibrium points the compositions are not at equilibrium and metastable. However, if one moves too far from the equilibrium it is possible to enter into the spinodal region, where the mixture is unstable. The spinodal region is defined where the free energy curve has an inflection point (points C and E). Within the spinodal region, any microscopic fluctuations (which are impossible to prevent) are sufficient to set up a chain reaction decomposing the composition into its equilibrium phases. Both the equilibrium compositions (binodal) and the spinodal region are defined by the free energy vs. composition curve. The binodal points (x, T) are those for which the first derivative of the Gibbs free energy of mixing is zero (minima). The

spinodal points (x, T) are those for which the second derivative of the Gibbs free energy of mixing is zero (inflection points).

Fig. 2.11 shows the molar enthalpy, entropy, and Gibbs free energy of mixing of two components when the enthalpy of mixing is positive and dominates the entropy term, calculated for $W = 25.7 \text{ kJ/mole}$ and $T = 484\text{K}$.

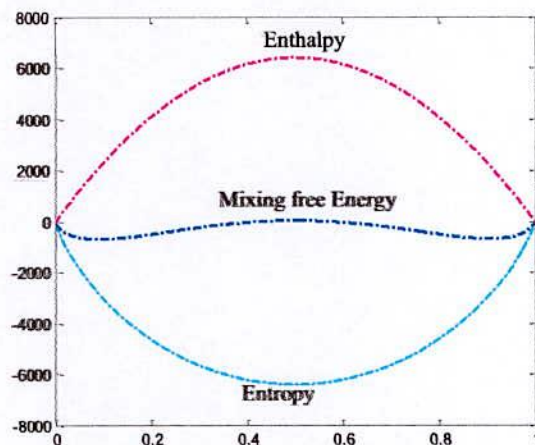


Fig-2.11 The enthalpy, entropy, and Gibbs free energy of mixing of $\text{In}_x\text{Ga}_{1-x}\text{N}$ calculated for $W = 25.7\text{KJ/mole}$ and $T = 484\text{K}$.

The Gibbs free energy of mixing is symmetrical about $x = 0.5$, at which point the entropy of mixing term produces a minimum and the enthalpy term produces a maximum. As can be seen, dG_{mix} is positive for almost all compositions making the binary system unstable at that temperature and completely immiscible.

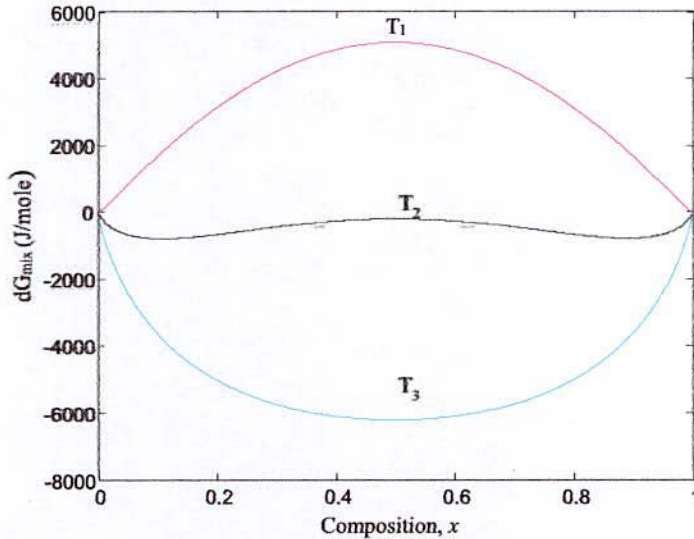


Fig. 2.12 Gibbs free energy of mixing for a regular solution calculated from equation (2.16) for different temperatures $T_1 < T_2 < T_3$ and $W = 25.7 \text{ kJ/mole}$.

At low temperature $T_1 = 100 \text{ K}$ the dG_{mix} curve has only a maximum and the system is completely immiscible. As the temperature increases to $T_2 = 500 \text{ K}$ the dG_{mix} curve has two minima and a maximum in between, which results in phase separation. At high temperatures $T_3 = 950 \text{ K}$ the entropy dominates and the system is fully miscible with dG_{mix} having only one minimum. The minimum value of T for which the system becomes fully miscible is called the critical temperature of solubility.

2.6 Phase Diagram of InGaN System

The boundary of the unstable region sometimes referred to as the binodal or coexistence curve is found by performing a common tangent construction of the free-energy diagram. The spinodal decomposition regions are defined as the regions that have negative curvature in the corresponding free energy versus composition curve. Inside the spinodal region the free energy

change is negative for small fluctuations in composition. The system is thus unstable and subject to composition fluctuations. As a result phase separation will occur. A more detailed overview of the phase diagrams of a binary alloy system including $\text{In}_x\text{Ga}_{1-x}\text{N}$ (pseudo-binary) is given in the next section. Phase separation in $\text{In}_x\text{Ga}_{1-x}\text{N}$ was first observed during growth of polycrystalline samples after long annealing at temperatures above 600°C [9]. Ho and Stringfellow [11] calculated a theoretical phase diagram for the InN – GaN alloy system (Fig. 2.13) using a modified valence force field model. This calculated phase diagram shows that the equilibrium solubility of InN in bulk GaN is approximately 6% at typical growth temperatures of 700 to 800°C . Phase separation through spinodal decomposition should occur in $\text{In}_x\text{Ga}_{1-x}\text{N}$ alloys containing more than 20% In at 800°C . These results were supported experimentally by El-Masry *et al.* [19] and by Ponce *et al.* [25]. X-ray diffraction (XRD) analysis and TEM indicated phase separation in $\text{In}_x\text{Ga}_{1-x}\text{N}$ layers with over 28% In composition grown by MOCVD. However, the calculations of Ho and Stringfellow [11] are done for relaxed $\text{In}_x\text{Ga}_{1-x}\text{N}$ material at equilibrium and as a result their phase diagram may not apply to strained $\text{In}_x\text{Ga}_{1-x}\text{N}$ layers.

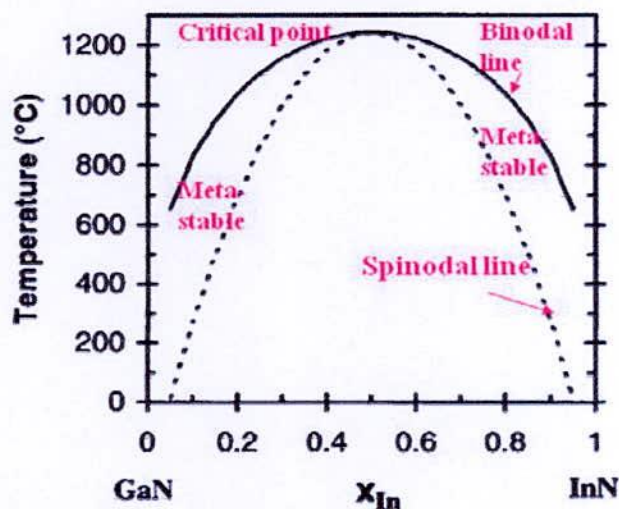


Fig. 2.13: Binodal (solid) and spinodal (dashed) curves for the $\text{In}_x\text{Ga}_{1-x}\text{N}$ alloys, calculated assuming a constant average value for the solid phase interaction parameter

The calculations of Karpov [14], for the phase diagram of biaxially strained $\text{In}_x\text{Ga}_{1-x}\text{N}$ produced a spinode with reduced miscibility gap and shifted toward higher indium contents than those predicted by Ho and Stringfellow [11]. The Karpov phase diagram is displayed in Fig 2.14 and

Fig 2.15 with including strain on phase diagram proposed by Ho and Stringfellow. Recent work by Liu and Zunger [17] also shows that phase separation may be suppressed by epitaxial strain. Some experimental support for the suppression of decomposition by epitaxial strain is provided by the work of Rao *et al.* [46] who studied $\text{In}_x\text{Ga}_{1-x}\text{N}$ epilayers more than 200 nm thick in TEM, and observed phase separation in relaxed regions of their films. However, regions of the films close to the $\text{In}_x\text{Ga}_{1-x}\text{N}/\text{GaN}$ interface did not show any evidence of phase separation.

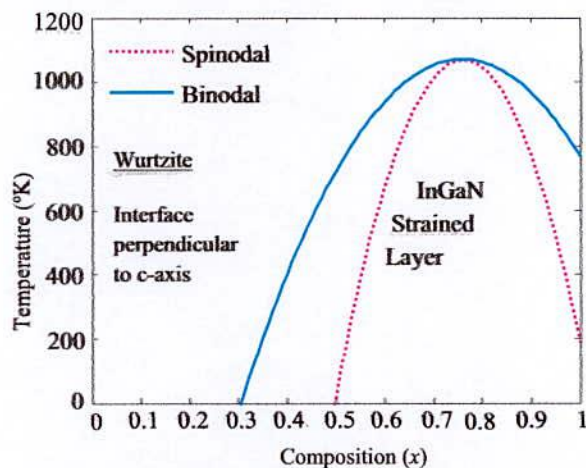


Fig. 2.14: T-x phase diagram of ternary $\text{In}_x\text{Ga}_{1-x}\text{N}$ alloys for strained layers with the interface orientation perpendicular to the hexagonal axis of the crystal.

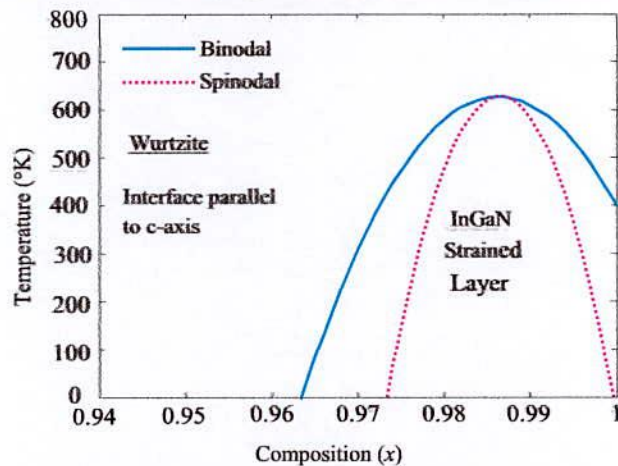


Fig. 2.15: T-x phase diagram of ternary $\text{In}_x\text{Ga}_{1-x}\text{N}$ alloys for strained layers with the interface orientation parallel to the hexagonal axis of the crystal.

Tabata *et al.*[47] also observed phase separation suppression in $\text{In}_x\text{Ga}_{1-x}\text{N}$ alloy layers due to external biaxial strain, while in the relaxed $\text{In}_x\text{Ga}_{1-x}\text{N}$ samples phase separation did occur. It is

also suggested that the composition pulling effect [46,48] plays an important role in suppressing phase separation around $\text{In}_x\text{Ga}_{1-x}\text{N}/\text{GaN}$ interfaces. The composition pulling effect limits In incorporation around interfaces due to the existence of large coherent strain. The lowered indium incorporation not only reduces the driving force for phase separation but also increases the critical thickness for relaxation. Upon growth, the layer progressively relaxes with more In incorporation, eventually triggering phase separation. Even though extensive research has been done in studying the InGaN material, most of the existing research is on strained films. No experimental data exist for freestanding InGaN material, which instigated the research that led to this work

2.7 Strained Films and Critical Thickness

The semiconductor thin film where the film is of different lattice constant than the substrate introduces strain. The strain energy containing in the film increases with the increase of thickness. If the film is thin enough to remain coherent to the substrate, then in the plane parallel to the growth surface, the thin film will adopt the in-plane lattice constant of the substrate. Fig.2.1 shows a substrate and a film with an equal and unequal lattice constant. The film is taken to be of larger lattice constant than the substrate e.g. InGaAs on GaAs or $\text{In}_x\text{Ga}_{1-x}\text{N}$ on GaN, and the top right illustration represents a thin coherent compressively strained film. The strain applied to the film by the substrate in the plane of the interface between the two is the result of biaxial compression. The lattice constant of the film in the direction perpendicular to the growth direction will likewise be strained according to the elastic properties of the film. It will either be smaller or larger than the unstrained value depending on whether the biaxial strain is tensile or compressive. However, if the film is thicker than the critical thickness, there will be sufficient strain energy in the film to create misfit dislocations to relieve the excess strain [5].

2.7.1 Different Models of Critical Thickness

In 1963 van der Merwe proposed a theory for the calculation of stresses at an interface between two adjacent crystals that have different lattice and/or elastic constants followed by his earlier work with Frank [49-51] and subsequent work for isotropic material [52]. Matthews and Blakeslee introduced a force balance model (MB model) in 1974 [53]. They investigated alternating layers of GaAs and GaAs_{0.5}P_{0.5} and revealed that, some threading dislocations

(TDs) experienced by misfit force and tension of dislocation line, bent back and forth in the layers interfaces, which gave rise to misfit dislocations. Though they have good agreement with experimental observation, some objections were raised. These were the driving force for further investigations and People-Bean published an article on the CT calculation based purely on an energy balance of the dislocation self-energy and the elastic energy which was compared with experimental results [54]. However, some drawbacks and uncertainties of their model were pointed out by Hu [55]. The story then continued with a semi-empirical model by Dodson and Tsao and studies of the excess stress for glide of a dislocation in a strained epitaxial layer by Freund-Hull and Fischer-Richter [56-58]. They proposed in a model which has been recently revised [59]. It is one of the “force models” and it was again discussed in detail by Holec [60]. Almost at the same time, calculations done by Willis et al., Jain et al. and Freund and Suresh based on the minimization of the overall energy appeared in the literature (energy balanced model) [61-63]. One of the advantages of the energy balanced (EB) model is that additional considerations of hexagonal symmetry such as GaN or more complex geometry can be incorporated in a straight forward manner. Therefore, mainly the EB model is used in this work. A brief summary of some commonly used model have been discussed in the subsequent sections.

2.7.2 Matthews and Blakeslee

The basis of this model is about two main forces, misfit force, F_a and the line tension, F_l acting on a preexisting dislocation in a strained film [53]. The stress field on the interfacial plane can expressed as

$$F_a = 2Gb h \epsilon_m \frac{1+\nu}{1-\nu} \cos \lambda \dots\dots\dots(2.17)$$

Where G is the shear modulus of the film, b is the magnitude of the burger vector of the misfit dislocation, h is the film thickness, ν is the Poisson’s ratio, λ is the angle between the burgers vector and the direction on the interfacial plane that is perpendicular to the dislocation line, ϵ_m is the lattice mismatch strain, whose value is $(a_f - a_s)/a_s$, where a_s and a_f are the lattice parameters of the substrate and the film, respectively. The second force on the misfit dislocation is due to the line tension, which acts like a restoring force, resisting the motion of the dislocation. This force (F_l) is given by

$$F_l = \frac{Gb^2(1-\nu \cos^2 \theta)}{4\pi(1-\nu)} \left[\ln\left(\frac{h}{r_0}\right) + 1 \right] \dots\dots\dots(2.18)$$

Here θ is the angle between the misfit dislocation line and its burgers vector. Therefore, total force acting on the dislocation, is $F_{total} = F_a + F_l$. For very small film thicknesses h , the total force F_{total} is negative and therefore acts against the extension (and possibly also against the creation) of the misfit dislocation. On the contrary, for sufficiently thick layers F_{total} is positive and thus the dislocation bends and create misfit segment. The CT is therefore determined by the equation $F_{total(hc)} = 0$, and in this equation ϕ is the angle between slip plane and normal to the film substrate interface and r_0 is dislocation cut-off parameter. Eqs. (2.17) and (2.18) yield the CT value as

$$h_c = \frac{b(1-\nu \cos^2 \theta)}{8\pi(1+\nu)|\varepsilon| \sin \theta \sin \phi} \ln\left(\frac{h_c}{r_0}\right) \dots\dots\dots(2.19)$$

2.7.3 People and Bean

On the contrary to the force balance model by Matthews and Blakeslee, People and Bean have approached the problem by balancing the overall energy. The stress field caused by misfit of the lattice parameters of the thin film and the substrate is generally a biaxial stress with the only non-zero components, $\sigma_{xx} = \sigma_{yy} = \sigma_m$, where σ_m is the misfit stress [54]. This is true for isotropic materials as well as for wurtzite materials where the interface is the c -plane (in which all directions are equivalent). According to this model, the strain energy per unit area of the film substrate interface is

$$E_m = 2G \frac{1+\nu}{1-\nu} \varepsilon_m^2 h \dots\dots\dots(2.20)$$

Taking the dislocation energy in the simplest possible case the “areal” energy of the dislocation with some characteristic width w is

$$E_d = \frac{l}{w} \frac{dE_d}{dl} = \frac{Gb^2(1-\nu \cos^2 \theta)}{4\pi(1-\nu)w} \ln\left(\frac{h}{r_0}\right) \dots\dots\dots(2.21)$$

People and Bean suggested that when E_d is exceeded by E_m , the misfit strain in the film will be replaced by misfit dislocations. By equating E_m and E_d one obtains the equation for the critical thickness h_c [58].

$$h_c = \frac{(1-\nu)}{(1+\nu)} \frac{b^2}{16\sqrt{2}\pi a(x)\epsilon^2} \ln\left(\frac{h_c}{r_0}\right) \dots\dots\dots(2.22)$$

The most remarkable feature of Eq. (2.22) is that there is a quadratic dependence on the misfit strain ϵ_m in contrast to Eq. (2.20) for the CT using the force balance model. This is a qualitatively different feature and thus one may expect very different curves of the CT against composition for these two models.

Chapter 3

Modeling for Growth Conditions of $\text{In}_x\text{Ga}_{1-x}\text{N}$ Epitaxial Layer

3.1 Introduction

In this chapter mathematical modeling of growth conditions for $\text{In}_x\text{Ga}_{1-x}\text{N}$ epitaxial layer has been developed considering prominent effect of various growth parameters such as group-III flow rate (TMI and TEG flow rate), molar ratio or $\text{TMI} / (\text{TMI} + \text{TEG})$, growth temperature, Indium composition in the epitaxial film, growth rate, group-V flow rate, group V/III ratio etc. Modeling algorithm as well as assumption that have been taken into account for evolving purpose has been mentioned in brief. Finally the developed model has been compared and fitted with the thermodynamically and experimentally obtained data found from different literature for its perfection and make this developed model applicable for the growth of phase separation free $\text{In}_x\text{Ga}_{1-x}\text{N}$ epitaxial layer with In composition up to 0.4.

3.2 Modeling of Growth Condition

A mathematical model is a description of a system using mathematical concepts and language. A perfect mathematical model is helpful to explain a system and to study the effect of different components influencing the system. By proper modeling one can make prediction about the behavior and output of the system. As mathematical model of MOVPE, the most widely used technique of growth of $\text{In}_x\text{Ga}_{1-x}\text{N}$ epitaxial film is not so available; sometimes it becomes very difficult to determine the rigorous effect of different growth parameters on epitaxial film. For this reason, it has been tried to develop a mathematical model for the growth of epitaxial film with an In composition up to 0.4 in case of MOVPE.

3.2.1 Modeling Assumption

$\text{In}_x\text{Ga}_{1-x}\text{N}$ epilayer that have been contemplated in this paper is assumed to be grown on (0001) sapphire substrates [64] by Metal Organic Vapor Phase Epitaxy (MOVPE) [9]. The $\text{In}_x\text{Ga}_{1-x}\text{N}$ epilayer is grown using the precursors TMI, TEG and ammonia (NH_3), with H_2 and N_2 as the carrier gas. The TEG and TMI sources were maintained at proper temperatures and pressures. Initially, about $2\mu\text{m}$ thick GaN templates were grown on (0001) sapphire at 1293K using Triethylgallium (TEG) and ammonia (NH_3) as the gallium and nitrogen sources, respectively. Then at 923K-1173K $\text{In}_x\text{Ga}_{1-x}\text{N}$ films are grown under properly maintained growth condition [9]. Here, consistent with the calculation by other researchers (the critical thickness of $\text{In}_x\text{Ga}_{1-x}\text{N}$ grown on GaN is about 100 nm [65,66]) some of the samples are over the critical thickness.

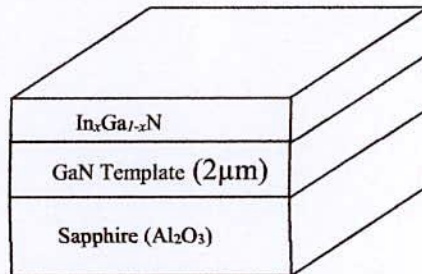


Fig. 3.1: Structure of hetero-epitaxial growth $\text{In}_x\text{Ga}_{1-x}\text{N}$.

3.2.2 Modeling

Indium (In) is typically believed to be a surfactant, producing smooth surface by changing the surface energy i.e. $\text{In}_x\text{Ga}_{1-x}\text{N}$ surface gets flatter if TMI flow get increased [12, 67]. TMI flow cannot also be very high because it risks the formation of In metal droplets[12,15]. Growth of $\text{In}_x\text{Ga}_{1-x}\text{N}$ is much more complicated by the fact that the mole fraction of Indium incorporated in the film, is not a simple function considering the relative input flow of TMI and TEG [68].

Figure 3.2 is a modeling diagram recounting composition, temperature and TMI flow rate that has been drawn considering [12, 16, 36, 68, 69]. Then it has been fitted with [16, 68, 70-72]. Through this model it has been anticipated that for a particular Indium composition in $\text{In}_x\text{Ga}_{1-x}\text{N}$

epitaxial film there is a relationship among the various growth parameters such as TMI, TEG and Ammonia flow rate, temperature, pressure, composition etc. If it is tried to grow a film of a particular composition, it is needed to know the relationship among the various parameters. A mathematical relationship has been developed that inter relates the different growth parameters.

$$T = 1.23 \times 10^3 - 69 \times \left(1 + 16.5x \frac{TEG}{TMI} \right)^{\frac{1}{2}} \dots\dots\dots(3.1)$$

Where x is the Indium composition in $In_xGa_{1-x}N$, T is the temperature (Kelvin), TMI and TEG are the flow rate ($\mu\text{mole}/\text{min}$). In this case, Ammonia flow rate have been considered constant.

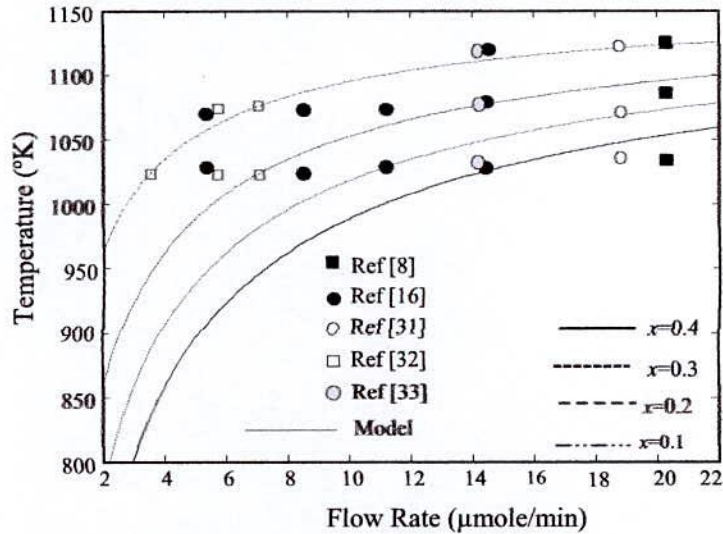


Fig. 3.2: Indium composition depending on TMI flow rate ($\mu\text{mole}/\text{min}$) and temperature ($^{\circ}\text{K}$).

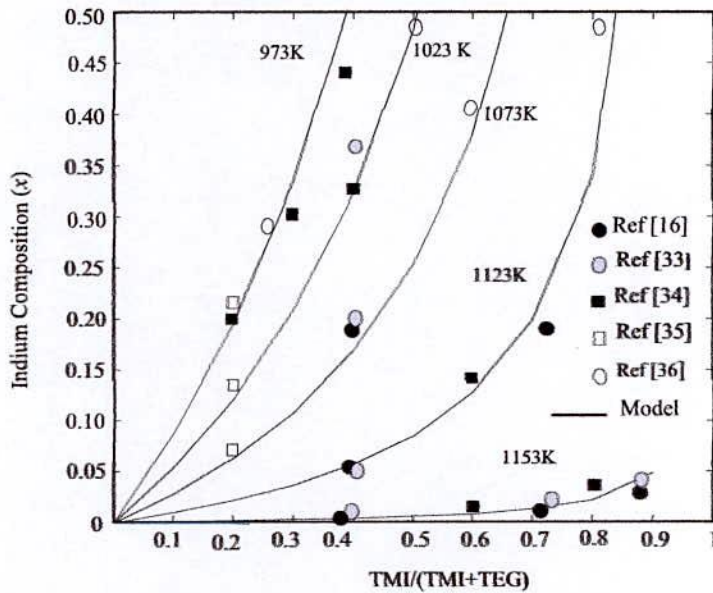


Fig. 3.3: In composition in the epitaxial layer as a function of molar ratio or gas phase mole fraction (TMI/TMI+TEG) with different growth temperatures (°K).

In order to conclude about the precision of developed model it has been compared with the thermodynamically and experimentally obtained data. The comparison of the data obtained from this model has become possible by making Indium composition as a function of Gas phase mole fraction (MR) or (TMI/(TMI+TEG)) and growth temperature. Now from equation (3.1), a mathematical relationship can be developed relating composition, gas phase mole fraction and temperature as follows:

$$x = \left\{ \left(\frac{1.23 \times 10^3 - T}{69} \right)^2 - 1 \right\} \frac{TMI}{16.5 \times TEG} \dots\dots\dots (3.2)$$

Figure 3.3 represents the Indium composition in $In_xGa_{1-x}N$ film according to equation (3.2) as a function of molar ratio for different temperatures with constant TEG flow rate. It shows very closeness to the thermodynamically obtained data [32-34] and physically [16, 70] that certifies the perfectness of our model. To justify this model as perfect, it has also been made a

relationship between Temperature and composition for other specific growth parameters. Composition decreases with temperature that can be obtained from our model. Equation (3.2) has been compared and fitted with [16, 31-33, 75] which shows very closeness to the experimentally obtained data.

Growth rate (G_R) is another fundamental parameter for the growth of high quality $In_xGa_{1-x}N$ epitaxial film. By assurance of properly maintained growth rate it is possible to grow epitaxial film without phase separation. Both structural and electrical properties were found to improve significantly with increasing G_R . The improvement in material quality is attributed to the suppression of phase separation with higher G_R [45]. The apt choice of growth rate helps to suppress the phase separation and inhomogeneity, thereby improves both the structural and electrical properties of $In_xGa_{1-x}N$ epilayer.

Table 3.1 represents the used typical values of different growth parameters including growth rate in different literatures for MOVPE growth of $In_xGa_{1-x}N$ epitaxy. Growth rate can be achieved as high as $5\mu\text{m/h}$ by MOVPE [17]. Due to very high growth rate there is a possibility of thermodynamic instability in the epitaxial film as well as it is very possible that high growth rate will results in inhomogeneous distribution and segregation of In atoms on the surface and lead to macroscopic domain with different In composition [36]. On the other hand, Lee et al. [16] reported that for lower growth rate, more uniform PL wavelength is found; these imply that the optical quality is improved and inhomogeneity decreases. Consequently, a lower growth rate is helpful to maintain a uniform composition in $In_xGa_{1-x}N$ layers [13]. But for lower growth rate the growing epitaxial films can spend relatively more time to order upon so there is a possibility of strain relaxation and there by occurrence of phase separation, formation of dislocation and other non-removable crystal defects. On the basis of above discussion and considering the used values of growth rate in different literatures from Table 3.1, typical range has been considered for developing the mathematical model of growth rate and it is from $0.1\mu\text{m/h}$ to $1.0\mu\text{m/h}$ for the growth of $In_xGa_{1-x}N$ epitaxy of In composition up to 0.4 by MOVPE.

Table-3.1 Typical Values of Growth rate and Other Growth Parameters used in Different Literatures for Different Indium Composition for the Case of $\text{In}_x\text{Ga}_{1-x}\text{N}$ Epitaxial Layer by MOVPE.

Composition x , (%)	Growth rate ($\mu\text{m/h}$)	Growth Pressure (Torr)	Growth Temperature ($^\circ\text{C}$)	V/III Ratio	Group-III Flow Rate		Ref.
					TEG or TMG ($\mu\text{mole/min}$)	TMI ($\mu\text{mole/min}$)	
7-14	0.03-0.58	100-500	660-780	20000-60000	3.10-18.00	1.11-52.53	[76]
12-49	NA	100-300	680-780	3000-10000	1-10	1-6	[77]
1-18	0.06-0.48	100	620-800	5000-17000	1-7	7-23	[31]
25-63	0.21-0.95	100-500	610-730	3000-15000	NA	NA	[45]
0-40	0.5	NA	750-900	4100-8600	23	3-15	[16]
16-53	0.13-0.14	150-500	760-840	5000-15000	NA	NA	[78]
10-40	NA	100-500	650-850	1400-4500	9	20-80	[68]

NA \rightarrow Not Applicable

In order to develop a mathematical modelling for growth rate for the growth of $\text{In}_x\text{Ga}_{1-x}\text{N}$ epitaxial film, at first it has been considered that growth rate as a function of growth temperature, growth pressure, group-III flow rate, group-V flow rate as well as taking into account the physical effect of molar ratio (TMI/TMI+TEG) and V/III ratio on the growth conditions. The growth rate decreases about linearly with increase of growth temperature [16, 25]. It has also been noted that due to increase in growth pressure growth rate starts to decrease [26, 27]. When the V/III ratio is increased the growth rate decreases because the relative input flow of the group-III precursors decreases. A mathematical relationship has been developed considering the dependency of growth rate on various growth parameters and physical growth condition [16-29].

$$G_R (\mu\text{mh}^{-1}) = \frac{TMI \times AMN^{-7/6}}{6.67 \times 10^{-4} P} \left\{ \left(\frac{1.23 \times 10^3 - T}{69} \right)^2 - \frac{TMI}{TEG} \right\} \dots\dots\dots (3.3)$$

Where AMN denotes group-V (ammonia) flow rate ($\mu\text{mole/min}$), P is growth pressure (atm).

3.2.3 Effect of Temperature on Growth Rate

Significant changes occur in the morphology of $\text{In}_x\text{Ga}_{1-x}\text{N}$ epitaxial layer due to the change in growth temperature. Growth rate as a function of growth temperature has been shown in Figure: 3.4 considering specific values of other growth parameters [33]. Growth rate decreases linearly with increasing growth temperature which is favorable for designing and fabrication of advanced devices with $\text{In}_x\text{Ga}_{1-x}\text{N}$ /GaN heterostructure [45]. It has been observed that growth rate can be changed by changing growth pressure and V/III ratio but the effectiveness of these parameters is found to be less pronounced as compared to the growth temperature.

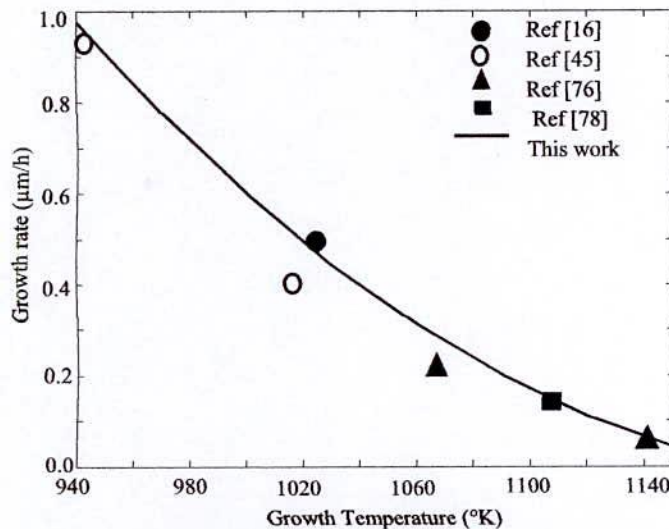


Fig. 3.4: Growth rate dependence on growth temperature with considering growth pressure =150 Torr and V/III ratio = 10000.

3.2.4 Effect of pressure on growth rate

Figure: 3.5 shows the effect of growth pressure on the growth rate for the specific values of other growth parameters. In this study, the total flow rate of the precursor as well as temperature of the reactor was kept same for the $\text{In}_x\text{Ga}_{1-x}\text{N}$ film growth under different growth pressure.

At low growth pressure the growth rate is high which may leads to instability in the grown film. On contrast, for high growth pressure the growth rate as well as In incorporation in the film

decreases considerably. The use of high growth pressure leads to a reduction in the surface roughness of the In incorporation in $\text{In}_x\text{Ga}_{1-x}\text{N}$ film [79].

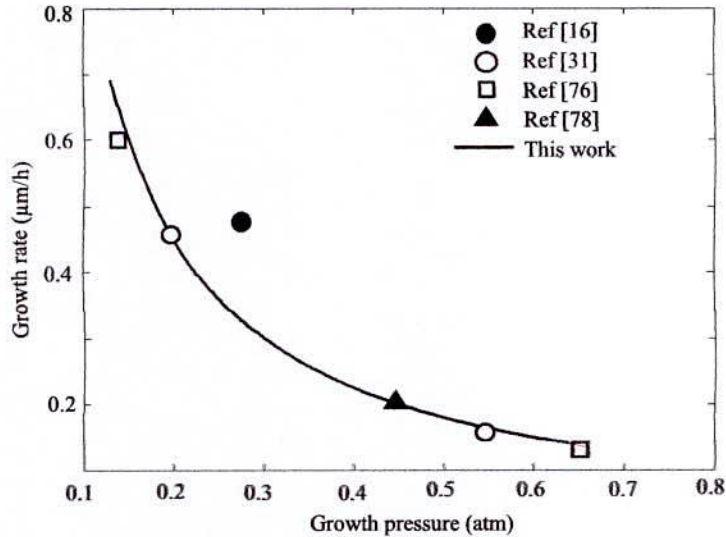


Fig. 3.5: Growth rate dependence on growth pressure with considering growth temperature =750°C and V/III ratio=10000.

3.2.5 Effect of V/III Ratio on Growth Rate

Figure 3.6 shows the effect of V/III ratio on the growth rate for epitaxial growth of $\text{In}_x\text{Ga}_{1-x}\text{N}$ film. In this particular study, the $\text{In}_x\text{Ga}_{1-x}\text{N}$ layers have been considered at 1023°K with constant growth pressure of 80Torr and the V/III ratio of the epitaxy was increased from 5000 to 12000. If growth rate is changed by varying the group III precursor flow there is a possibility of change in the In composition in $\text{In}_x\text{Ga}_{1-x}\text{N}$ epitaxial film [79] because due to the variation in group III flow, variations occur in the mole fraction which is the basic parameter for interacting with Indium incorporation in the film at constant temperature. Also the V/III ratio should not be very high because surface roughness increases with increasing in V/III molar precursor ratio, indicating a degradation of surface quality [80].

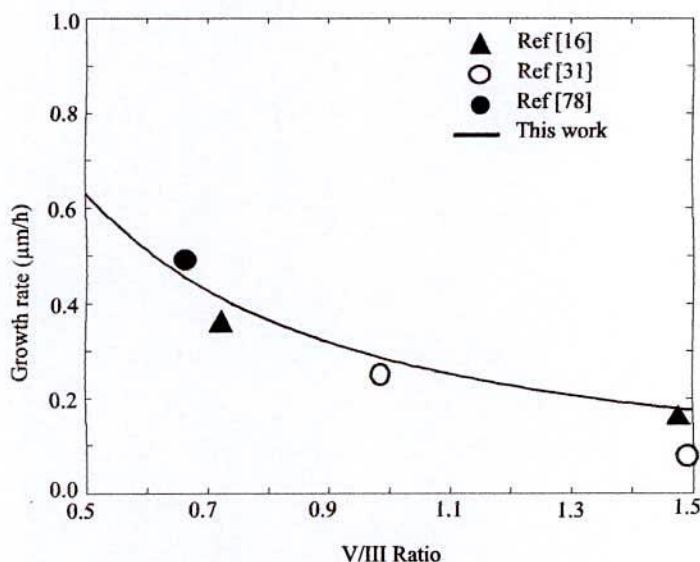


Fig. 3.6: Growthrate dependency on V/III ratio with considering growth temperature 750 °C and growth pressure 150 Torr.

3.3 Theoretical Investigation for Growth Temperature

From Gibb's free energy equation it is clear that mixing free energy is dependent on enthalpy and entropy. If enthalpy is constant (in case of constant composition and interaction parameter) then mixing free energy is totally dependent on entropy where entropy is directly dependent on temperature. The determination of approximate value of this temperature is a crucial issue for the growth of $\text{In}_x\text{Ga}_{1-x}\text{N}$ epitaxial film of expected In composition. A modified thermodynamic analysis may be helpful to overcome this difficulty. In the prevailed analysis, phase separation for the $\text{In}_x\text{Ga}_{1-x}\text{N}$ ternary system has been analyzed using a strictly regular solution model. According to these calculated results, the critical temperature for $\text{In}_x\text{Ga}_{1-x}\text{N}$ is found to be 1236°C but the practical observations are different from this value. The mixing free energy of $\text{In}_x\text{Ga}_{1-x}\text{N}$ should be negative than the mixing free energy of InN and GaN otherwise $\text{In}_x\text{Ga}_{1-x}\text{N}$ separated into two phase. The mixing free energy is dependent on temperature and interaction energy that has been observed in the above analysis as discussed in details in chapter 2. On the other hand high temperatures are desirable for growth of nitride films in order to dissociate ammonia (NH_3) and free up nitrogen for bonding. The InN bond is significantly weaker than that for GaN at high temperatures, and $\text{In}_x\text{Ga}_{1-x}\text{N}$ films will tend to have difficulty with In

incorporation. If the temperature is lowered, hydrogen will etch nitrogen away from the In leaving In droplets on the growth surface. By taking all above if we consider a typical value of free energy for $\text{In}_x\text{Ga}_{1-x}\text{N}$ epitaxy at which this epitaxy is more stable and the modified Valance Force Field method is used then the equation for growth temperature can be written as

$$T = \frac{-[5700 + Wx(1-x)]}{R[x \ln(x) + (1-x) \ln(1-x)]} \dots\dots\dots(3.4)$$

The interaction parameter used in the analysis is obtained from a strain energy calculation using the valence force field model [28].

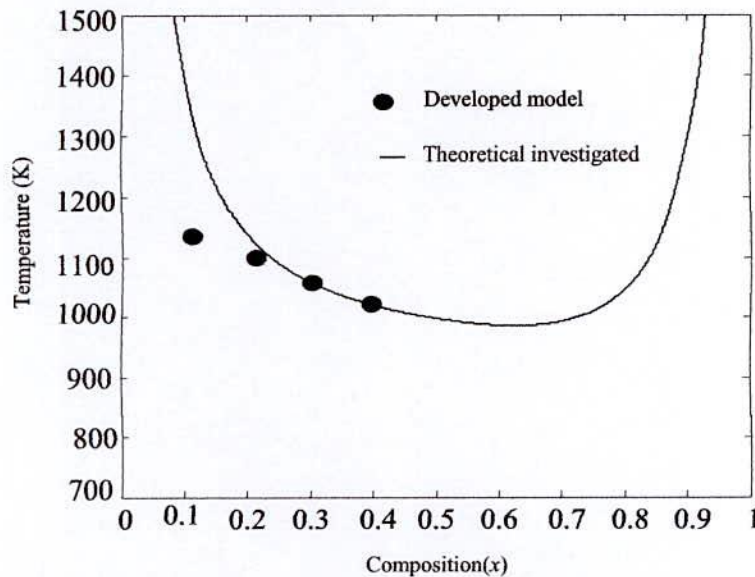


Fig-3.7: Dependency of composition (x) on the growth temperature of $\text{In}_x\text{Ga}_{1-x}\text{N}$.

Figure 3.7 shows the theoretical investigation to determine the precision of developed model. It is possible to determine the approximate value of growth temperature for any composition ($x=0\sim 0.4$) for a range of molar ratio (0.27 to 0.50) from the developed model. For particular value of molar ratio (0.50) the required temperatures for different composition obtained from the

above developed model has been fitted with the thermodynamically obtained data. After fitting both of the data it is found that these show the very closeness to each other.

3.4 Strain and Compositional Analysis

Due to the different lattice constants of GaN and InN the $\text{In}_x\text{Ga}_{1-x}\text{N}$ films will grow under biaxial compressive strain. The magnitude of strain will depend on the alloy's mole fraction, layer thickness and other growth parameters. For $\text{In}_x\text{Ga}_{1-x}\text{N}$, strain influencing optical properties, seems to play a role in the incorporation of the indium itself [81]. The strains produced by the difference of the lattice constants or the thermal expansion coefficients between two materials are commonly known not to relax but to be accommodated in a pseudomorphically grown film. On the contrary, the strains in a layer with thickness greater than the critical value begin to relax, generating defects such as dislocations and three-dimensional growth. The effects of strain on In incorporation in MOVPE films have been qualitatively studied by Hiramatsu et al [82]. Also various groups such as S. U. Karpov [10], Ho and Stringfellow [11] analyzed the effect of strain on film quality of $\text{In}_x\text{Ga}_{1-x}\text{N}$. So far, there has not been any systematic study addressing the strain behavior in $\text{In}_x\text{Ga}_{1-x}\text{N}$ film, mainly due to the difficulty in separating the effects of strain and composition on the lattice constants.

In-plane strain increases with the increase of indium composition in $\text{In}_x\text{Ga}_{1-x}\text{N}$ epitaxial layer of a particular thickness. It has also been noted that in-plane strain decreases with increasing in layer thickness [83-88]. RBS and depth resolved cathode luminescence (CL) measurements indicate that the In content is not uniform over depth in same samples. This phenomenon generally occurs in the case of strained layers which suggest that the strain is a driving force for compositional pulling effect. Due to this effect band gap variation occurs in the epitaxial layer that decreases the quality and deteriorates the device performance.

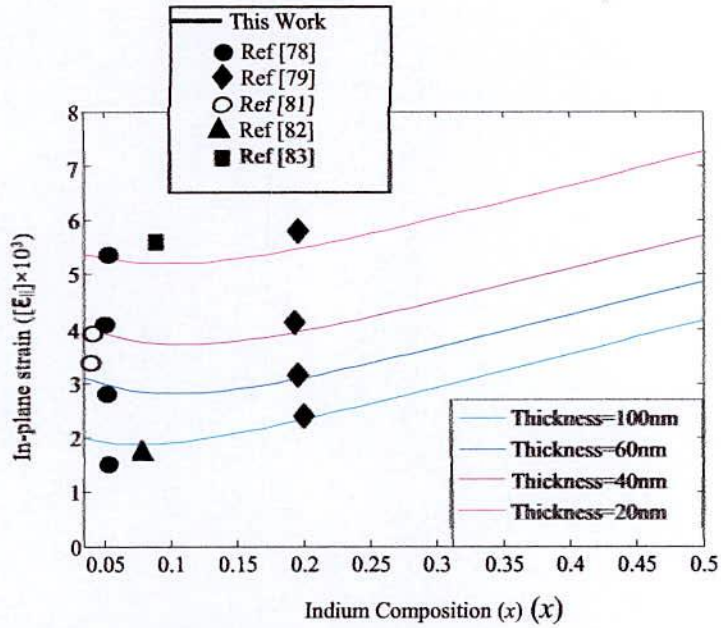


Fig. 3.8: Plotting and modelling of In-plane strain in $\text{In}_x\text{Ga}_{1-x}\text{N}$ epitaxial layer as a function of layer thickness and indium composition (x).

Taking into account these rigorous effects on epitaxial film quality a mathematical modeling has been developed based on experimental value obtained from different literatures as shown in Fig 3.8.

$$h = 33.68 \left(1 + 1.15 \exp^{-16.67x} \ln \left(\frac{1 + 3.42 \times 10^{-3} \exp^{-11.12x}}{x + 16.13 \varepsilon_{II} - 12.156 \times 10^{-3}} \right) \right) \dots\dots\dots(3.5)$$

To verify this model, In-plane strain has been made as a function of epilayer thickness and indium composition incorporated to this layer. Then it has been fitted with [83,84] and Matthews, Mader, and Light Kinetic Model (Quantitative Models for Lattice Relaxation)[88] as shown in Figure 3.9. It is found that this modeling is a good agreement with the experimental observation.

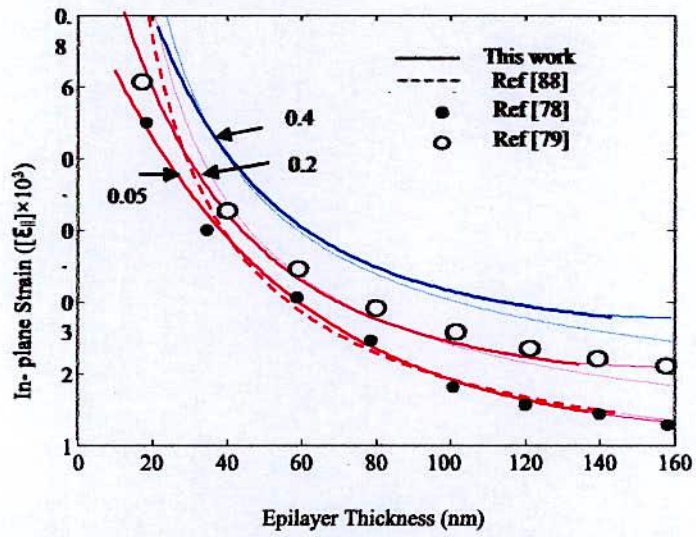


Fig. 3.9: In plane strain variation with Epilayer thickness and the verification of developed model.

Chapter 4

Results and Discussion

4.1 Introduction

The developed model is expected to be promisingly applicable and superior for the growth of $\text{In}_x\text{Ga}_{1-x}\text{N}$ epitaxial film of particular In composition without phase separation under the influence of various growth parameters. It will be very helpful to acquire a preceding idea about the growth conditions i.e. required limiting values of different growth parameters and anticipated quality of the epitaxial film before the growth commence. The main objective of this chapter is to study and analysis the result obtained from this developed model. Finally a phase diagram has been proposed by the help of this developed model as well as considering the result bring into being from the other literatures related to this field under the evolution of In composition up to 0.4.

4.2 Temperature Dependence of In Composition in $\text{In}_x\text{Ga}_{1-x}\text{N}$ Epitaxial Film

Temperature is one of the most noteworthy growth parameter because significant changes occur in the morphology of $\text{In}_x\text{Ga}_{1-x}\text{N}$ epitaxial layer due to the change in growth temperature. In composition in the grown film as a function of growth temperature has been shown in Fig. 4.1 considering specific values of other growth parameters.

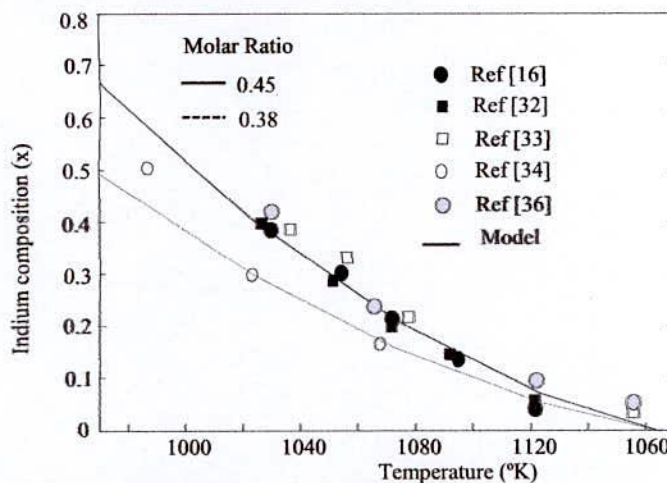


Fig 4.1: In composition in the epitaxial film for different temperatures and TMI / (TMI+TEG).

Almost In composition decreases linearly with increase in growth temperature which is favorable for designing and fabrication of advanced devices with $\text{In}_x\text{Ga}_{1-x}\text{N}$ /GaN heterostructure [44]. It has been found from this developed model that with the increase in growth temperature In composition in $\text{In}_x\text{Ga}_{1-x}\text{N}$ epitaxial film linearly decreases with a particular value of molar ratio which supports about the precision of this developed model without any difficulty.

4.3 Phase Diagram

Deposition of Indium nitride (InN) in $\text{In}_x\text{Ga}_{1-x}\text{N}$ epitaxial film is very difficult during the growth at high temperature. It has been reported that $\text{In}_x\text{Ga}_{1-x}\text{N}$ alloys are unstable over most of the composition range at normal growth temperature [8]. The reason is that at high temperatures, most of the input Ga (Gallium) deposits into the solid phase, whereas In remains in the vapor phase without deposition. So it is very important to determine the range of the growth parameters for particular In composition in $\text{In}_x\text{Ga}_{1-x}\text{N}$ epitaxial film. In order to specify the growth parameter for particular In composition (0~0.4) a diagram, in Fig. 4.2, has been anticipated which has been drawn by considering the boundary condition of equation (3.2) as well as comparing with physical system and experimental data. To interpret this diagram, composition curve has been drawn for different TMI and TEG flow rate and concerning other growth parameters such as Ammonia flow rate, Gas phase mole fraction, temperature etc.

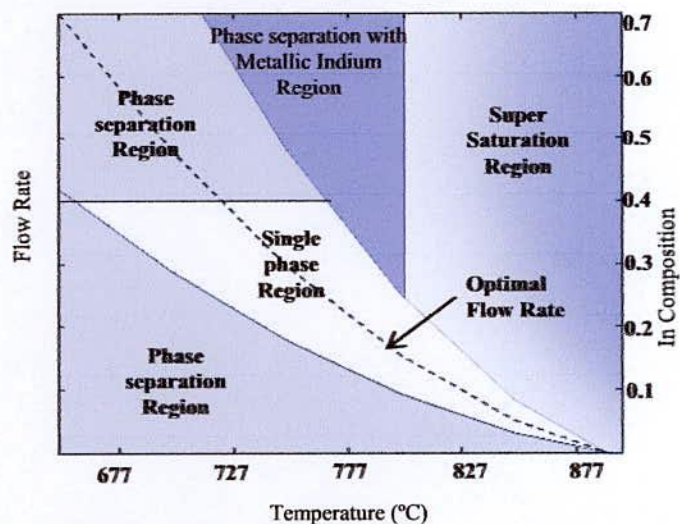


Fig. 4.2: Approximation of the growth parameters for the growth of $\text{In}_x\text{Ga}_{1-x}\text{N}$ concerning molar ratio, In composition and growth temperature.

It has been reported that the surface of $\text{In}_x\text{Ga}_{1-x}\text{N}$ epitaxial film gets unsmooth as the TMI flow decreases [12]. There is also a possibility of phase separation due to relatively low TMI flow [41, 66]. From X-Ray Diffraction (XRD), it is clear that when for molar ratio is less than 0.27; there is the evidence of phase separation [9]. For these conditions mentioned above the compositional region obtained in the diagram has been discarded with relatively low density gray color which is illustrated in Fig. 4.2. When the growth of $\text{In}_x\text{Ga}_{1-x}\text{N}$ film is carried out at a relatively low temperature ($\leq 1073\text{K}$) with a relatively high TMI / (TMI+TEG) (>0.50), there is a possibility of metallic In incorporation in the $\text{In}_x\text{Ga}_{1-x}\text{N}$ epitaxial film [61, 63]. Considering this effect on growth condition a region has been identified in this diagram with relatively deep gray color showing phase separation with metallic In incorporation.

In contrast, at high growth temperature In composition in solid is almost independent of the TMI / (TMI+TEG) and gradually decreases with increase in growth temperatures [49]. Due to high evaporation rate of In, the super saturation happens i.e. In incorporation gets saturated and starts to decrease. Meanwhile, the decomposition of In-N bonds takes place [8] i.e. although TMI / (TMI+TEG) gets increased but composition remains approximately unchanged. A super saturation region has been identified by graded gray color. Furthermore concern of this model is up to composition 0.4; the region which is greater than the range interested has been discarded.

Growth rate ($\mu\text{m h}^{-1}$) has made as a function of temperature, gas phase mole fraction and group-III flow rate. The value of growth rate for all values of TMI / (TMI+TEG) is not acceptable. The limiting values of TMI and TEG for getting TMI / (TMI+TEG) in the acceptable range for the growth of $\text{In}_x\text{Ga}_{1-x}\text{N}$ epitaxial layer of In composition up to 0.4 have been accepted from [9, 10]. For a given TMI flow rate and TMI / (TMI+TEG) the TEG flow rate can be estimated. For the given values of TMI, for the corresponding molar ratio gives the value of TEG.

Figure 4.3 shows the dependency of growth rate on growth temperature for different molar ratio. It also includes In composition in $\text{In}_x\text{Ga}_{1-x}\text{N}$ epitaxial film for different growth rate and temperature. Here temperature has been varied from 970K to 1150K. Normally growth rate is controlled by changing the V/III ratio with constant molar ratio for a particular In composition. From the above model it is easily obtainable the specific value of growth rate for a particular In composition. From the Fig. 4.3, it is seen that it is possible to grow phase separation free $\text{In}_x\text{Ga}_{1-x}$.

xN epitaxial film of a particular In composition for specific value of molar ratio. For obtaining specific value of molar ratio the specific values of precursor flow rate has to be selected from the help of approximation diagram as shown in Figure 4.2. In figure 4.3 growth rate varies with increase in TEG flow rate as well as TMI flow rate. When both of them are increased the growth rate also increases. The empty circle indicates the growth rate as line where molar ratio is 0.27, the solid circles correspond to molar ratio 0.50 and empty triangular shape indicates growth rate in the line at molar ratio of 0.38. At a glance overview shows that the favorable growth region decreases with increase in growth temperatures. Finally it can be concluded that this developed model will be very helpful for a researcher to grow high quality and phase separation free $In_xGa_{1-x}N$ epitaxial films of any arbitrary In composition up to 0.4.

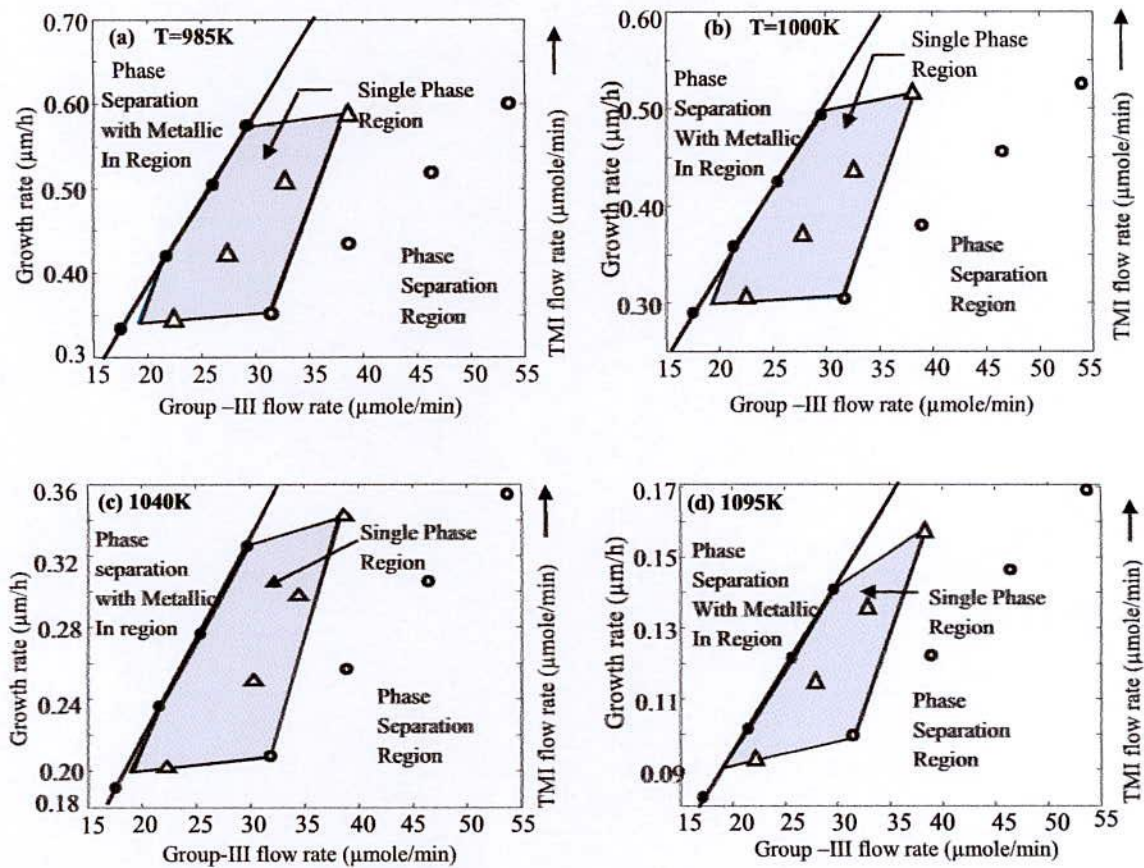


Fig. 4.3: Favorable growth region as a function growth temperatures, group-III flow rate and molar ratio.

To understand the in-plane strain effect on phase separation, binodal and spinodal decomposition curve of $\text{In}_x\text{Ga}_{1-x}\text{N}$ at fully relaxed state has been taken into consideration. It has been observed that the spinodal curve starts to shift towards higher In content with increasing in-plane strain. But the in-plane strain decreases with increasing film thickness. On the other hand, it has been found from other experimental results that the critical thickness of $\text{In}_x\text{Ga}_{1-x}\text{N}$ film decreases with increasing In content. From this point of view, it has been included the critical layer thickness in binodal and spinodal decomposition curve. Alternately it can be concluded that the spinodal curve starts to shift towards lower In composition with increasing critical layer thickness as the numerical value of the fully strained state decreases with relatively lower In incorporation in the $\text{In}_x\text{Ga}_{1-x}\text{N}$ Epitaxy.

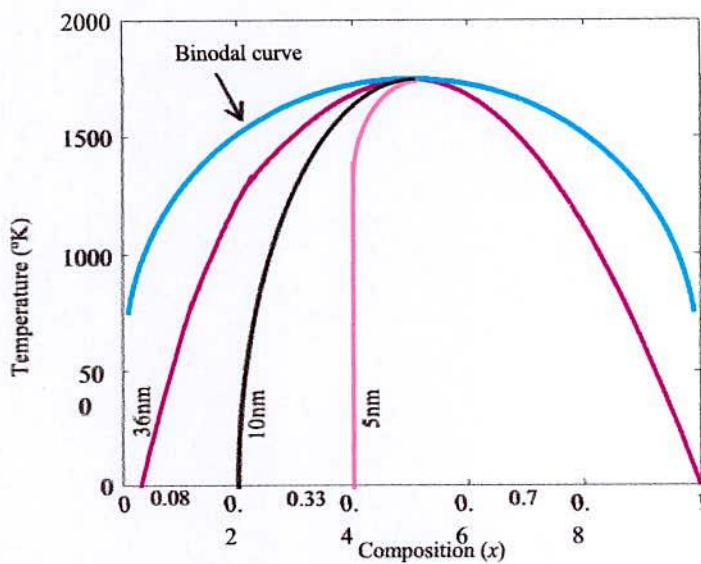


Fig. 4.4: Phase diagram of the Spinodal decomposition in $\text{In}_x\text{Ga}_{1-x}\text{N}$ / GaN epitaxial film of different thickness for strained and relaxed condition.

Chapter 5

Conclusion and Future work

5.1 Conclusion

The growth of high quality In-rich $\text{In}_x\text{Ga}_{1-x}\text{N}$ film is a major concern due to its wide range of application. Phase separation which causes low performance of $\text{In}_x\text{Ga}_{1-x}\text{N}$ based device can be reduced by controlling various growth parameters. In this dissertation, the phase separation suppression technique for wuzrite as well as cubic heteroepitaxy has been investigated through theoretical studies and the estimation of growth conditions of MOVPE growth of $\text{In}_x\text{Ga}_{1-x}\text{N}$ ($x \sim 0.4$) epitaxial layer has been performed. Here, a model has been developed showing the dependence of phase separation occurred in $\text{In}_x\text{Ga}_{1-x}\text{N}$ film on different growth parameters. The developed model has been compared and fitted with the thermodynamically and experimentally obtained data found from different literature for its perfection. Through this model it has been shown that $\text{In}_x\text{Ga}_{1-x}\text{N}$ film of any arbitrary Indium composition up to 0.4 can be grown without phase separation as well as metallic Indium incorporation. When $\text{TMI}/\text{TMI}+\text{TEG}$ is greater than 0.5, although the Indium composition increases but there is a possibility of metallic Indium incorporation up to temperature 800°C . When temperature is greater than 800°C Indium composition get saturated and not affected by increase in $\text{TMI}/\text{TMI}+\text{TEG}$ rather decreases with increase in temperature only. Also it is well-known that for low $\text{TMI}/\text{TMI}+\text{TEG}$, the surface quality and optical properties of the film goes to deteriorate. Lowest $\text{TMI}/\text{TMI}+\text{TEG}$ has been ranged without phase separation is 0.27.

In-plane strain is another dominant parameter for controlling phase separation. In this work this strain also has been interpreted in binodal and spinodal curve of $\text{In}_x\text{Ga}_{1-x}\text{N}$ epitaxy in order to include critical layer thickness in the phase diagram at different Indium composition. Another modeling has been developed showing the dependence of in-plane strain on film thickness and indium composition. The proposed model provides a good agreement with another theoretical model.

5.2 Future Work

This study gives a mathematical modeling for the growth of $\text{In}_x\text{Ga}_{1-x}\text{N}$ epitaxial film concerning the rigorous effects of various growth parameters that greatly influences the quality of the epitaxial film. In spite of this, the modeling involves some limitations viz. all the growth parameters and factors that affect the quality of the epitaxial film have not been taken into consideration. So, the phase diagram that has been anticipated in this modeling permits the growth of $\text{In}_x\text{Ga}_{1-x}\text{N}$ epitaxial film up to 40% indium composition without phase separation. If it is possible to draw a phase diagram considering the other factors such as effect of buffer layer, effect of carrier gas and polarization effect on film quality then it would be possible to fabricate phase separation free $\text{In}_x\text{Ga}_{1-x}\text{N}$ epitaxial film for higher indium incorporation.

References

- [1] J. Wu, W. Walukiewicz, K. M. Yu, J. W. Ager III, E. E. Haller, H. Lu, and W. J. Schaff, Small band gap bowing in $\text{In}_{1-x}\text{Ga}_x\text{N}$ alloys, *Appl. Phys. Lett.* 80 (2002) 4741-4743.
- [2] K. Mukose, M. Sano, Theoretical study of composition fluctuation in InGaN films on various substrates, *J. Phys. Conf. Ser.* 152 (2009) 012025.
- [3] Md. Rafiqul Islam, Md. Tanvir Hasan, A. G. Bhuiyan, M. R. Islam and A. Yamamoto, Design and performance of InGaN-based MJ solar cells, *IETECH J. of Electrical Analysis*, 2(4) (2008) 237-243.
- [4] Nakamura, S., et al., Characteristics of $\text{In}_x\text{Ga}_{1-x}\text{N}$ multi-quantum-well-structure laser diodes. *Applied Physics Letters*, 68(23): (1996). p. 3269
- [5] S. Nakamura, *The blue laser Diode*. 1997, Springer.
- [6] K. Fuji, K. Kusakabe, and K. Ohkawa, Photo electrochemical properties on $\text{In}_x\text{Ga}_{1-x}\text{N}$ for H_2 generation from aqueous water, *Jpn. J. Appl.Phys.* 44 (2005) 7433-7435.
- [7] J. Wu, W. Walukiewicz, K. M. Yu, W. Shan, J. W. Ager, E. E. Haller, H. Lu, W. J. Schaff, W. K. Metzger, and S. Kurtz, Evolution of phase separation in In-rich InGaN alloy, *J. Appl. Phys.* 94 (2003) 6477-6479.
- [8] Y. Guo, X.L. Liu, H.P. Song, A.L. Yang, X.Q. Xu, G.L. Zheng, A study of indium incorporation in In-rich InGaN grown by MOVPE, *Applied Surface Science* 256 (2010) 3352-3356
- [9] K. Osamura, S. Naka, and Y. Murakami, *J. Appl. Phys.*, Vol.46, 3432 (1975).
- [10] Jianghai Zheng, Junyong Kang, Theoretical study of phase separation in wurtzite InGaN, *Materials Science in Semiconductor Processing* 9 (2006) 341-344
- [11] I. H. Ho and G. B. Stringfellow, Solid phase immiscibility in GaInN, *Appl. Phys. Lett.* 69 (1996) 2701-2703.
- [12] Yong Huang, Omkar Jani, Eun Hyun Park, and Ian Ferguson, Influence of growth conditions on phase separation of InGaN bulk materials grown by MOCVD, *Mater. Res. Soc.* 955 (2007).

- [13] O. K. Jani, Development of Wide-Band Gap InGaN Solar Cells for High-Efficiency Photovoltaics, Ph D Thesis, Georgia Institute of Technology, Atlanta, Georgia, (2008).
- [14] S. Y. Karpov, Suppression of phase separation in InGaN due to elastic strain, *MRS Internet J. Nitride Semicond. Res.* 3 (1998) 16-22.
- [15] Yong Huang, Omkar Jani, Eun Hyun Park, and Ian Ferguson, Influence of growth conditions on phase separation of $\text{In}_x\text{Ga}_{1-x}\text{N}$ bulk materials grown by MOCVD, *Mater. Res. Soc.* 955 (2007).
- [16] Md. Rafiqul Islam, Md. Rejvi Kaysir, Md. Jahirul Islam, A Hasihmoto, A Yamoto, MOVPE Growth of $\text{In}_x\text{Ga}_{1-x}\text{N}$ ($x \sim 0.4$) and Fabrication of Homo Junction Solar Cell, *J. Mater. Sci. Tech.* 29(2), (2013) 128-136.
- [17] J. Z. Liu and A. Zunger, Thermodynamic states and phase diagram for bulk-incoherent, bulk-coherent and epitaxially-coherent semiconductor alloy: Application to cubic (Ga,In)N, *Phys. Rev. B* 77 (2008) 205201-205212.
- [18] R. Singh, D. Doppalapudi, T. D. Moustakas, and L. T. Romano, *Appl. Phys. Lett.* 70, 1089 (1997).106.
- [19] N. A. El-Masry, E. L. Piner, S. X. Liu, and S. M. Bedair, *Appl. Phys. Lett.* 72,40 (1998).
- [20] M. D. McCluskey, L. T. Romano, B. S. Krusor, D. P. Bour, N. M. Johnson, and S. Brennan, *Appl. Phys. Lett.* 72, (1998) 1730.
- [21] P. Ruterana, G. Nouet, W. Van Der Stricht, I. Moerman, and L. Considine, *Appl. Phys. Lett.* 72, (1998) 1742.
- [22] D. Doppalapudi, S. N. Basu, K. F. Ludwig, and T. D. Moustakas, *J. Appl. Phys.* 84, (1998) 1389.
- [23] D. Doppalapudi, S. N. Basu, and T. D. Moustakas, *J. Appl. Phys.* 85, (1999) 883.
- [24] M. K. Behbehani, E. L. Piner, S. X. Liu, N. A. El-Masry, and S. M. Bedair, *Appl. Phys. Lett.* 75, (1999) 2202.
- [25] F. A. Ponce, S. Srinivasan, A. Bell, L. Geng, R. Liu, M. Stevens, J. Cai, H. Omiya, H. Marui, and S. Tanaka, *Phys. Stat. Sol. B* 240, (2003) 273-284.

- [26] Z. Liliental-Weber, D. N. Zakharov, K. M. Yu, J. W. Ager III, W. Walukiewicz, E. E. Haller, H. Lu, and W. J. Schaff, *Physica B* **376-377**, 468(2006).
- [27] N. Weiser, O. Ambacher, H.-P. Felsl, L. Görgens, and M. Stutzmann, *Appl. Phys. Lett.* **74**, (1999) 3981.
- [28] F.A. Ponce, and D. P. Bour, *Nature* **386**, (1997) 351.
- [29] L. Teles, J. Furthmüller, L. Scolfaro, J. Leite, and F. Bechstedt, "Influence of composition fluctuations and strain on gap bowing in $\text{In}_x\text{Ga}_{1-x}\text{N}$," *Phys. Rev. B* **63**, (2001) 085204.
- [30] F. Bechstedt, J. Furthmüller, M. Ferhat, L. Teles, L. Scolfaro, J. Leite, V. Davydov, O. Ambacher, and R. Goldhahn, "Energy gap and optical properties of $\text{In}_x\text{Ga}_{1-x}\text{N}$," *Phys Status Solidi A* **195**, (2003) 628–633.
- [31] Yong Huang, Jae-Hyun Ryou, Andrew Melton, Muhammad Jamil, Balakrishnam Jampana, Russell D. Dupuis, Growth and characterization of InGaN alloys by metal organic vapor deposition for solar cell application, *J. Photon. Energy* . **2**(1) (Feb 23, 2012), 028501.
- [32] M. Horie, K. Sugita, A. Hasimoto, A. Yamamoto, *Solar Energy Materials and Solar Cells*, **93** (2009) 1013-1015.
- [33] Akinori Koukitu, Naoyuki Takahashi, Tetsuya Taki, Hisashi Seki, Thermodynamic analysis of the MOVPE growth of $\text{In}_x\text{Ga}_{1-x}\text{N}$, *Journal of Crystal Growth* **170** (1997) 306-311.
- [34] S. Yu. Karpov, Advances in the modeling of MOVPE processes, *Journal of Crystal Growth* **248** (2003) 1-7.
- [35] Yoshihiro Kangawaa, Tomonori Itob, Yoshinao Kumagaia, Akinori Koukituaa, Thermodynamic study on compositional instability of InGaN/GaN and InGaN/InN during MBE, *Applied Surface Science* **216** (2003) 453–457.
- [36] Keunjoo Kim and Sam Kyu Noh, Reactor design rules for GaN epitaxial layer growths on sapphire in metal-organic chemical vapour deposition, *Semicond. Sci. Technol.* **15** (2000) 868.
- [37] A. Koukitu, N. Takahashi, and H. Seki, *Jpn. J. Appl. Phys., Part 2* **36**, L1136 (1997).
- [38] C. H. Chen, Z. M. Fang, G. B. Stringfellow, and R. W. Gedridge, *J. Appl. Phys.* **69**, (1991) 7605.

- [39] A. Koukitsu, T. Taki, N. Takahashi, and H. Seki, *J. Cryst. Growth* 197,(1999) 99.
- [40] K. L. Choy, *Handbook of nanostructured materials and nanotechnology*, vol.1, synthesis and processing, Academic Press, San Diego, CA, P533 (2000).
- [41] K. L. Choy, *Progress in Materials Science* 48,(2003) 57.
- [42] K. Sasamoto, T. Hotta, K. Sugita, A.G. Bhuiyan, A. Hashimoto, A. Yamamoto, K. Kinoshita, Y. Kohjib, MOVPE growth of high quality p-type InGaN with intermediate In compositions *Journal of Crystal Growth*, 318 (2011) 492-495.
- [43] S. Pereira, M. Correia, E. Pereira, K. O'Donnell, E. Alves, A. Sequeira, N. Franco, I. Watson, and C. Deatcher, "Strain and composition distribution in wurtzite InGaN/GaN layers extracted from x-ray reciprocal space mapping," *Appl. Phys. Lett.* 80,(2002) 3913–3915
- [44] J.P. Liu, R.Q. Jin, J.J. Zhu, J.C. Zhang, J.F. Wang, M. Wu, Effects of TMIn flow on the interface and optical properties of InGaN/GaN multiple quantum wells, *J. of Cryst. Growth* 264 (2004) 53–57.
- [45] B. N. Pantha, J. Li, J. Y. Lin and H. X. Jiang, Single phase $\text{In}_x\text{Ga}_{1-x}\text{N}$ ($0.25 \leq x \leq 0.63$) alloys synthesized by metal organic chemical vapor deposition, *Appl Phys. Lett.* 93, (2008) 182107.
- [46] M. Rao, D. Kim, and S. Mahajan, *Appl. Phys. Lett.* 85, (2004) 1961.
- [47] A. Tabata, L. K. Teles, L. M. R. Scolfaro, J. R. Leite, A. Kharchenko, T. Frey, D. J. As, D. Schikora, K. Lischka, J. Furthmuller and F. Bechstedt, *Appl. Phys. Lett.* 80, 769 (2002).107
- [48] K. Hiramatsu, Y. Kawaguchi, M. Shimizu, N. Sawaki, T. Zheleva, R. F. Davis, H. Tsuda, W. Taki, N. Kuwano, and K. Oki, *MRS Internet J. Nitride Semicond. Res.* 2, (1997) 6.
- [49] F. C. Frank, and J. H. van der Merwe, "One-dimensional dislocations. I. Static theory," *Proc. R. Soc. London, Ser. A, Mathematical and Physical Science*, Vol. 198, No.1053, (1949) pp.205-216.
- [50] F. C. Frank, and J. H. van der Merwe, "One-dimensional dislocations. II. Misfitting monolayers and oriented overgrowth," *Proc. R. Soc. London, Ser. A, Mathematical and Physical Science*, Vol. 198, No.1053,(1949) pp.216-225.

- [51] J. H. van der Merwe, "Crystal interfaces. Part I. Semi-infinite crystals," *Journal of Applied Physics*, Vol. 34, Issue 1,(1963) pp. 117-122.
- [52] J. H. van der Merwe, "Crystal interfaces. Part II. Finite overgrowths," *Journal of Applied Physics*, Vol. 34, Issue 1,(1963) pp. 123-127.
- [53] J. W. Matthews, and A. E. Blakeslee, "Defects in epitaxial multilayer: 1. Misfit dislocation," *Journal of Crystal Growth* 27, pp. 118-125 (1974).
- [54] R. People, and J.C. Bean, "Calculation of critical layer thickness versus lattice mismatch for $GexSi_{1-x}/Si$ strained-layer heterostructures," *Applied Physics Letter*, Vol. 47, Issue 3, (1985) pp.322-324.
- [55] S. M. Hu, "Misfit dislocations and critical thickness of heteroepitaxy," *Journal of Applied Physics*, Vol. 69, Issue 11, (1991) pp. 7901-7903.
- [56] B. W. Dodson, and J. Y. Tsao, "Relaxation of strained-layer semiconductor structures via plastic-flow," *Applied Physics Letter*, Vol. 51, Issue 17, (1987) pp. 1325-1327.
- [57] L. B. Freund, and R. Hull, "On the Dodson-Tsao excess stress for glide of a threading dislocation in a strained epitaxial layer," *Applied Physics Letter*, Vol. 71, Issue 4, (1992) pp. 2054-2056.
- [58] A. Fischer, and H. Richter, "On plastic flow and work hardening in strained layer heterostructures," *Applied Physics Letter*, Vol. 64, Issue 10, (1994) pp. 1218-1220.
- [59] A. Fischer, "Stability constraints in SiGe epitaxy" In J. D. Cressler, editor, *Silicon Heterostructures Handbook – Materials, Fabrication, Devices, Circuits, and Applications of SiGe and Si Strained-Layer Epitaxy* CRC Press, Taylor & Francis Group, Boca Raton chapter 2.7 (2006) pp. 127-143.
- [60] D. Holec, "Critical thickness calculations for $In_xGa_{1-x}N/GaN$ systems," CPGS thesis, University of Cambridge/Selwyn College (2006).
- [61] J. R. Willis, S. C. Jain, and R. Bullough, "The energy of an array of dislocations implications for strain relaxation in semiconductor heterostructures," *Phil. Mag. A*, Vol. 62, Issue 1, (1990) pp. 115-129.
- [62] S. C. Jain, A. H. Harker, and R. A. Cowley, "Misfit strain and misfit dislocations in lattice mismatched epitaxial layers and other systems," *Phil. Mag. A*, Vol. 75, (1997) pp. 1461-1515.

- [63] L. B. Freund, and S. Suresh, "Thin film materials: stress, defect formation, and surface evolution," Cambridge University Press, Cambridge, (2003).
- [64] L. Gorgens, O. Ambacher, M. Stutzmann, C. Miskys, F. Scholz and J. Off, Characterization of InGaN thin films using high-resolution X-Ray diffraction, *Appl. Phys. Lett.* 76 (2000) 577-579.
- [65] D. Holec, P.M.F.J. Costa, M.J. Kappers, C.J. Humphreys, Critical thickness calculations for InGaN/GaN, *J. Cryst. Growth* , 303 (2007) 314–317.
- [66] M. Leyser, J. Stellmach, Ch. Meissner, M. Pristovsek, M. Kneissl, The critical thickness of InGaN on (0 0 0 1) GaN, *J. Cryst. Growth* 310 (2008) 4913–4915.
- [67] H. Chen, R. M. Feenstra, J. E. Northrup, T. Zywietz, J. Neugebauer, and D. W. Greve, Surface structures and growth kinetics of InGaN(0001) grown by molecular beam epitaxy, *J. Vac. Sci. Technol. B* 18 (2000) 2284-2289.
- [68] Y. Guo, X.L. Liu, H.P. Song, A.L. Yang, X.Q. Xu, G.L. Zheng, A study of indium incorporation in In-rich InGaN grown by MOVPE ,*Applied Surface Science* 256 (2010) 3352–3356.
- [69] H. Chen, R. M. Feenstra, J. E. Northrup, T. Zywietz, J. Neugebauer, and D. W. Greve, Surface structures and growth kinetics of InGaN(0001) grown by molecular beam epitaxy, *J. Vac. Sci. Technol. B* 18 (2000) 2284-2289.
- [70] K. Sasamoto, T. Hotta, K. Sugita, A.G. Bhuiyan, A. Hasimoto, A. Yamamoto, MOVPE growth of high quality p-type InGaN with intermedite Indium composition, *J. Cryst. Growth* 318 (2011) 492-495.
- [71] A. Pretorius, T. Yamaguchi, C. K"ubel, R. Kr"oger, D. Hommel, and A. Rose-nauer, "Structural investigation of growth and dissolution of $\text{In}_x\text{Ga}_{1-x}\text{N}$ nano-islands grown by molecular beam epitaxy," *J. Cryst. Growth* 310, (2008) 748–756.
- [72] M. Schuster, P.O. Gervais, B. Jobst, W. H"osler, R. Averbeck, H. Riechert, A. Iberl, and R. St"ommer, "Determination of the chemical composition of distorted InGaN/GaN heterostructures from x-ray diffraction data," *J. Phys. D: Appl. Phys.* 32, (1999) A56–A60
- [73] L. Vegard, "Die Konstitution der Mischkristalle und die Raumf"ullung der Atome," *Z. Phys.* 5, (1921) 17–26.
- [74] O. Ambacher, M. S. Brandt, R. Dimitrov, T. Metzger, M. Stutzmann, R. A. Fischer, A. Miehler, A. Bergmaier, and G. Dollinger, *J. Vac. Sci. Technol. B* 14, (1996) 3532.
- [75] J. B. McChesney, P. M. Bridenbaugh, and P. B. O'Connor, *Mater. Res. Bull.* 5, (1970) ,783

- [76] K. Jacobs, B. Van Daele, M.R. Leys, I. Moerman, G. Van Tendeloo, "Effect of growth interrupt and growth rate on MOVPE-grown InGaN/GaN MQW structures", *Journal of Crystal Growth* 248, (February.2003) pp. 1461-1515.
- [77] Mark K Behbehani, "Study of Phase Separation and Ordering in InGaN and AlInGaN: Experimental and Computer Modeling", Phd Thesis, North Carolina State University, 2004.
- [78] Veit Hoffmann, "MOVPE growth and characterization of (In,Ga)N quantum structures for laser diodes emitting at 440 nm", Berlin 2011.
- [79] Rachel A. Oliver, Menno J. Kappers, and Colin J. Humphreys, G. Andrew D. Briggs, Growth modes in heteroepitaxy of InGaN on GaN, *J. Appl. Phys* 97, (2005) 013707.
- [80] G. Durkaya, M. Buegler, R. Atalay, I. Senevirathna, M. Alevli, O. Hitzemann, M. Kaiser, R. Kirste, A. Hoffmann and N. Dietz, The influence of the group V/III molar precursor ratio on the structural properties of InGaN layers grown by HPCVD, *Phys. Status Solidi A* 207, No. 6, (2010) 1379–1382.
- [81] Sérgio Pereira, Maria. R. Correia, Estela Pereira, C. Trager-Cowan, F. Sweeney, P.R. Edwards, K.P. O'Donnell, E. Alves, A.D. Sequeira, N. Franco, Strain and Compositional Analysis of InGaN/GaN Layers, *Mat. Res. Soc. Symp Vol. 639* © 2001 Materials Research Society.
- [82] K. Hiramatsu et al, *MRS Internet J. Nitride Semicond. Res.*, 2(1997) 6.
- [83] Hirth, J. P. and Lothe, J., *Theory of dislocations*, Krieger Publishing Company, Malabar, Florida, 2nd ed., 1982.
- [84] Hull, D. and Bacon, D. J., *Introduction to Dislocations*, Butterworth-Heinemann, Oxford, reprint of 4th ed. 2002.
- [85] Seong-Eun Parka, Byung-sung O, Cheul-Ro Lee, Strain relaxation in $\text{In}_x\text{Ga}_{1-x}$ N epitaxial films grown coherently on GaN, *Journal of Crystal Growth* 249 (2003) 455–460.
- [86] Z. Liliental-Weber, K. M. Yu, M. Hawkrige, S. Bedair, A.E. Berman, A. Emara, D. R. Khanal, J. Wu, J. Domagala, and J. Bak-Misiuk, Structural perfection of InGaN layers and its relation to photoluminescence *Phys. Status Solidi C* 6, No. 12, (2009) 2626 – 2631.

[87] Sérgio Pereira^a, Maria. R. Correia^a, Estela Pereira^a, C. Trager-Cowan^b, F. Sweeney^b, P.R. Edwards^b, K.P. O'Donnell^b, E. Alves^c, A.D. Sequeira^c, N. Franco^c, Strain and Compositional Analysis of InGaN/GaN Layers, *Mat. Res. Soc. Symp.* Vol. 639 © 2001 Materials Research Society.

[88] J.P. Liu, R.Q. Jin, J.J. Zhu, J.C. Zhang, J.F. Wang, M. Wu, Effects of TMIn flow on the interface and optical properties of InGaN/GaN multiple quantum wells, *J. of Cryst. Growth* 264 (2004) 53–57

[89] Ohn E. University of Connecticut, Storrs, CT, "Heteroepitaxy of semiconductors theory, growth and characterization". Ayers